THE ASTROPHYSICAL JOURNAL, 418:812–831, 1993 December 1

LITHIUM ABUNDANCES AND OTHER CLUES TO ENVELOPE BURNING IN SMALL MAGELLANIC CLOUD ASYMPTOTIC GIANT BRANCH STARS

BERTRAND PLEZ,[1] VERNE V. SMITH,[2] AND DAVID L. LAMBERT[3]
Astronomy Department and McDonald Observatory, University of Texas at Austin, Austin, TX 78712-1083
Received 1993 April 21; accepted 1993 June 8

ABSTRACT

We present a chemical analysis of seven luminous asymptotic giant branch stars and one M supergiant of the Small Magellanic Cloud. The abundances are derived from high-resolution spectra by spectrum synthesis using new, spherically symmetric, opacity sampling model atmospheres. The average metallicity is [Fe/H] = −0.5, in accordance with other determinations of the SMC's metallicity. The AGB stars show signs of envelope burning, being Li rich, C poor, and with a low $^{12}C/^{13}C$ ratio. The *s*-process elements (Rb, Zr, Nd) abundance pattern is different from that in the solar system, and is characteristic of a high exposure at low neutron density. This is not peculiar to the SMC, however, but seems to be an effect of metallicity: Galactic Ba, CH, and S-type stars at the same metallicity display similar *s*-process element abundance patterns. Apparently, the ^{13}C neutron source is operating in these intermediate-mass thermally pulsing AGB stars.

Subject headings: Magellanic Clouds — nuclear reactions, nucleosynthesis, abundances — stars: AGB and post-AGB

1. INTRODUCTION

The Magellanic Clouds have long provided key opportunities for the study of stellar evolution. Due to the fact that the distances to the Clouds are well determined, accurate luminosities can be derived for stars in both the Small and Large Clouds (SMC and LMC). In particular, investigations into the late stages of stellar evolution have benefited from surveys of red giants in the Clouds. Surveys of both "oxygen-rich" (C/O < 1) M, MS, and S stars (e.g., Wood, Bessell, & Fox 1983, hereafter WBF; Hughes 1989; see the review by Wood, Moore, & Hughes 1991) and carbon (C/O > 1) stars (e.g., Westerlund et al. 1978; Blanco, McCarthy, & Blanco 1980; Rebeirot, Azzopardi, & Westerlund 1993) provide hundreds of candidates for more detailed studies via high-resolution spectroscopy.

Many of these late-type M, MS, S, and C stars surveyed in the Clouds are examples of stars evolving along the asymptotic giant branch (AGB). The AGB stars are post ^{4}He-core burning objects which consist of an electron-degenerate C-O core, around which a H-burning shell operates, and a deep, outer convective envelope. Below the H-burning shell, ^{4}He burns periodically into ^{12}C through a thermal runaway in a shell surrounding the degenerate core. The large amount of energy released through triple-α burning in this runaway drives a convective shell, which extinguishes the H-burning shell, and leads ultimately to the mixing of ^{12}C throughout this interior region of the star. As energy is carried away and the thermal runaway dies, the H-burning shell is reestablished and the deep, outer convective envelope mixes ^{12}C-rich material to the star's surface. In addition, during these thermal runaways, neutrons are liberated by either the $^{13}C(\alpha, n)^{16}O$ or $^{22}Ne(\alpha, n)^{25}Mg$ reactions and these neutrons produce the neutron-rich heavy elements which characterize the *s*-process (such as Zr or Ba). These ^{4}He thermal runaways have been labeled thermal pulses (TPs) and much of the picture described above is based on the work of Schwarzschild & Härm (1967), Sanders (1967), Uus (1973), Iben (1975, 1981), and Truran & Iben (1977). The periodic mixing of ^{12}C and heavy-element *s*-process species into the atmosphere of an AGB star will eventually transform an M giant into a ^{12}C- and *s*-process–rich S or C star.

A significant challenge to the theory of stellar evolution was the apparent "cutoff" luminosity for carbon stars in the Clouds: very few C stars were found brighter than $M_{bol} = -6$, although the stellar models predicted numerous C stars extending up to the AGB limit of $M_{bol} \approx -7.1$ (see the detailed review by Iben & Renzini 1983). A possible solution to this puzzling discrepancy between theory and observation was provided by WBF's (1983) discerning observation that many of the luminous long-period variables (LPVs) within the luminosity interval of $-7 \lesssim M_{bol} - 6$ in the Clouds are probably S stars, i.e., O-rich rather than C-rich stars with absorption bands of ZrO in their spectra. The ZrO bands suggested to WBF that these stars were luminous TP-AGB candidates which had dredged *s*-process elements to their surfaces. TP-AGB stars presumably also dredge ^{12}C from the He-shell to their surfaces. WBF speculated that the luminous MS and S stars remained O-rich by burning some of the ^{12}C added to the envelope into ^{14}N via the CN cycle. This step requires that the base temperature of the convective envelope be hot enough to burn ^{12}C through CN cycle ($T_{base} \gtrsim 20 - 40 \times 10^6$ K). Such stellar models have been investigated by Scalo & Ulrich (1973), Iben (1973), Sackmann, Smith, & Despain (1974), Scalo, Despain, & Ulrich (1975, hereafter SDU), Renzini & Voli (1981), and Sackmann & Boothroyd (1992): this primary production of ^{14}N in the outer convective envelope has been dubbed "envelope burning."

A prediction of some of these models (SDU; Sackmann & Boothroyd 1992) is that envelope burning leads to the production of ^{7}Li in the envelope via the "^{7}Be transport mechanism" (Cameron & Fowler 1971). Luminous TP-AGB stars identified by WBF

[1] E-mail: I: plez@astro.as.utexas.edu.
[2] Visiting Astronomer, Cerro Tololo Inter-American Observatory. CTIO is operated by AURA, Inc., under contract to the National Science Foundation. E-mail: verne@astro.as.utexas.edu.
[3] Visiting Astronomer, Anglo-Australian Telescope. E-mail: dll@astro.as.utexas.edu.

were investigated using high-resolution spectroscopy by Smith & Lambert (1989, 1990a), who found that all of the luminous O-rich AGB stars brighter than $M_{bol} \approx -6$ exhibited strong Li I λ6707 lines, and interpreted the enhanced Li abundances estimated for these stars as the signature of envelope burning.

In this paper, we investigate in detail eight stars from the SMC. Seven of the octet are AGB S stars (WBF) with a strong Li I λ6707 line and enhanced lines of heavy elements (Smith & Lambert 1989, 1990a). The eighth star is not an AGB star but a massive supergiant of higher luminosity than the S stars but at a similar effective temperature and with obviously a much weaker Li I λ6707 line and weaker Zr I and Nd II lines than the S stars. For this paper, we have analyzed high-resolution spectra from 6500 to 8800 Å and low-resolution infrared 2 (μm) spectra, using state-of-the-art model atmospheres and synthetic spectra. Our emphasis is on certain measures of the chemical compositions that offer especial clues to the evolution of AGB stars:

1. The Li abundance is obtained from the strong Li I λ6707 and the weak subordinate line at 8126 Å;
2. The $^{12}C/^{13}C$ ratio (and the C abundance) is estimated from the CO vibration-rotation bands near 2.2 μm;
3. The Zr and Nd, as well as the iron-group Cr, Fe, Co, and Ni abundances are derived from a "window" between molecular bands at 7400–7600 Å;
4. The Rb abundance is estimated from the Rb I λ7800 resonance line.

Our results for the Li abundance and the $^{12}C/^{13}C$ ratio are used to test the hypothesis that the luminous AGB stars experience "envelope burning." The Zr, Nd, and especially the Rb abundance provide insights into the operation of the *s*-process in the He-burning shell. In particular, the Rb/Zr ratio is predicted to increase by a factor of $\sim$10 as the neutron density at which the *s*-process operates is increased from below to above 10^9 cm^{-3}. Certain extant models of the He-shell predict neutron densities above 10^9 cm^{-3}. These predictions may, in principle, be tested using measurements of the Rb and Zr abundances.

2. OBSERVATIONS

Most spectra were obtained at the Cerro Tololo Inter-American Observatory (CTIO) with the 4 m telescope and two spectrometers: the cassegrain echelle cross-dispersed spectrometer and the infrared spectrometer (IRS). The data used in this study were obtained over three separate observing runs in 1988 July, 1989 November, and 1990 November. Echelle spectra were taken with the red air-Schmidt camera and GEC 386 × 576 CCD detector at two wavelength settings. In 1988 July and 1989 November spectra from 6500 to 7900 Å were obtained, which contain the resonance Li I doublet: these spectra comprised the data set used in the initial survey papers of Smith & Lambert (1989, 1990a). During 1990 November, additional echelle spectra were taken to cover the range 7700–8800 Å, primarily to observe the weaker and less-blanketed Li I 8126 line, and the Rb I λ7800 resonance line. This additional Li I line is used to improve our estimate of the Li abundance for a selected set of SMC stars. The echelle spectra have resolutions of $R = \lambda/\Delta\lambda \approx 20{,}000$ and typical S/N ratios of 50–150. In addition, the star N371:C12 was observed near 7800 Å at the Anglo-Australian Observatory 3.8 m telescope with the coudé spectrometer known as UCLES, at a resolution of $\sim$50,000. The spectra were reduced from two-dimensional frames to single-order one-dimensional spectra using IRAF. Also, the Galactic M-supergiant Betelgeuse, as well as 12 other M supergiants from the Per OB1 and Cyg OB2 associations, were observed near 7800 Å as comparisons for the Rb I line in the SMC red giants. These spectra were taken with the McDonald Observatory's 2.7 m telescope plus coudé spectrometer with a Texas Instrument 800 × 800 CCD. The resolution here was 41,000.

During two nights at CTIO in 1990 November, the IRS was used to gather low-resolution ($R \approx 2000$) IR spectra of the 2 μm CO bands in five of the SMC stars for which we had 6707 and 8126 Å Li I observations. The detector used was a 58 × 62 pixel Santa Barbara Research Corporation indium-antimonide array. The CO bands of interest are the ^{12}CO (2–0) band at 2.2935 μm and the ^{12}CO (4–2) and ^{13}CO (2–0) bands at 2.3524 and 2.3448 μm, respectively. As the chip can only record 0.036 μm of spectrum, two grating tilts were required: we chose one tilt at 2.29621 μm to record the ^{12}CO (2–0) band and the other at 2.34467 μm to observe both the ^{13}CO (2–0) and the ^{12}CO (4–2) bands. Sky background was significant and the observing sequence at each grating setting consisted of sky-object-sky-object-sky exposures, followed by a zenon comparison lamp for wavelength calibration. Interpolated sky frames were subtracted from each object frame in the data reduction. On both nights a hot star near the SMC (HR 338–B6V + B9V) was observed about every 45 minutes and used to ratio out telluric absorption features from our SMC spectra. On each night, 15 flat-field frames were taken at both the beginning and end of the night: these flat fields were taken by observing the dome white spot at 3.3 μm through an *L* filter, as routinely done at the CTIO. IRAF was used to produce wavelength-calibrated one-dimensional spectra of sky-subtracted, flat-fielded images. Telluric features were removed by dividing the SMC program stars by a spectrum of HR 338 interpolated to the mean airmass of the program spectra: a linear interpolation of HR 338 spectra was used and the telluric features were removed to high accuracy.

In Table 1 we list the program SMC stars studied here as well as the dates of the observing runs on which particular spectral regions were observed. We also note which stars are the "Li-strong" objects. In Figure 1 we illustrate the region near the Li I resonance doublet for the SMC M-supergiant NGC 371 star C12 (which we denote N371:C12) and the SMC S-star HV 11223. Other than the differences in the Li I doublet, the spectra look fairly similar. We show more examples of spectra and of synthetic fits in § 4.

3. ANALYSIS AND RESULTS

3.1. *Model Atmospheres and Basic Data*

Our analysis combines state-of-the-art line-blanketed model atmospheres and synthetic spectroscopy with extensive line lists. It is not possible to use an equivalent width approach due to the strong veiling by molecular lines. The model atmospheres were calculated with the SOSMARCS code of Plez, Brett, & Nordlund (1992). This code is a much enhanced version of the venerable MARCS (Gustafsson et al. 1975). The models are flux constant, line-blanketed, hydrostatic, spherically symmetric, in LTE, with a

TABLE 1

PROGRAM SMC STARS

Star	6707 Å	8126 Å	2 μm	Li I Strong
HV 11223	1988 Jul	1990 Nov	1990 Nov	Yes
HV 1963	1988 Jul	1990 Nov	1990 Nov	Yes
HV 11366	1988 Jul	1990 Nov	...	Yes
HV 12179	1988 Jul	1990 Nov	1990 Nov	Yes
HV 11329	1989 Nov	1990 Nov	...	Yes
HV 1375	1988 Jul	1990 Nov	...	Yes
HV 11452	1989 Nov	1990 Nov	1990 Nov	Yes
N371:C12	1989 Nov	1990 Nov	1990 Nov	No

mixing-length description of convection and a full opacity sampling treatment of all opacities. The major opacity sources for M-type giants have been included, with some newly calculated H_2O, TiO and VO (see Plez et al. 1992 for more details). The synthetic spectra were generated with an enhanced version of the "Spectrum" program package originally developed at Uppsala Observatory. The new version ("TurboSpectrum") shares much of its input data and routines with SOSMARCS (e.g., the continuous opacities and the spherical transfer routines) and can handle millions of lines in reasonable amounts of time. The program has been tested against the widely used MOOG (Sneden 1973), and no significant differences have been found.

Line lists for the different spectral regions of interest in the optical (6665–6735 Å, 7655–7770 Å, 7390–7590 Å, 7775–7835 Å, and 8075–8180 Å) were assembled in the following way: for TiO, all lines for the ^{48}TiO isotope were taken ($v = 0$ to 15, $J = 0$ to 200) from the predictions of Plez et al. (1992) with a change in the *gf*-values of the γ and γ' systems based on new lifetime measurements by Doverstål & Weijnitz (1992). The factor applied to the *gf*-values were 0.88 for γ' and 0.56 for γ, based on early results from this group (Lindgren 1991). The actual values derived from their final assessment of the lifetimes are 0.81 ± 0.06 for γ' and 0.52 ± 0.02 for γ. However, this difference is negligible with regard to other sources of uncertainty. No lines were included from other isotopes of Ti or O. The calculated wavelengths are sufficiently accurate for our purpose, but the wavelengths of some strong lines (e.g., around the 6707 Å Li I line) were adjusted when they could be found in the compilation of laboratory measurements of Phillips (1988).

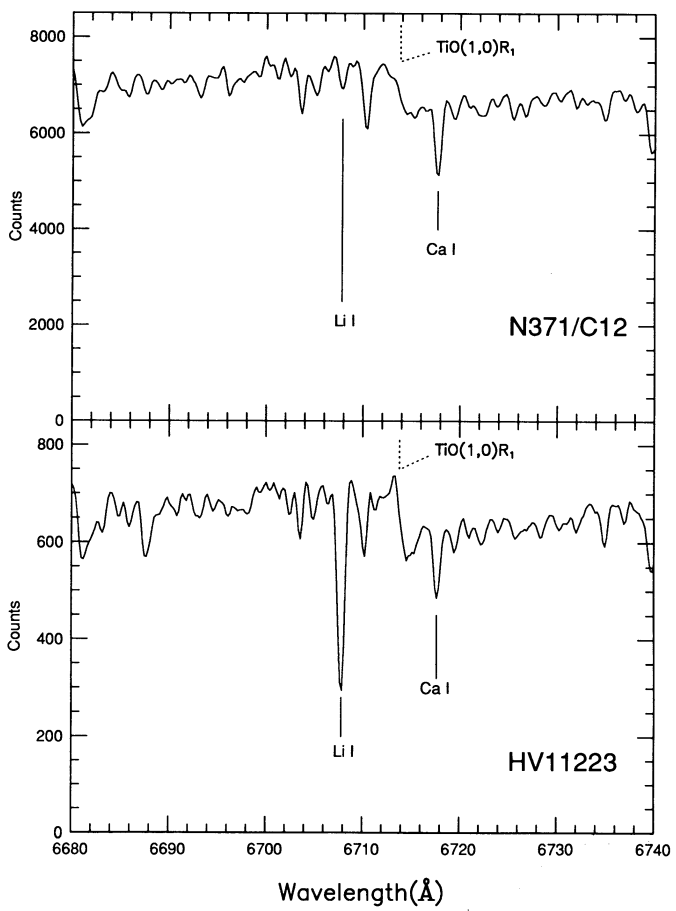

FIG. 1.—Illustration of the large difference in the Li I line-strengths between (*top*) the M-supergiant N371:C12 and (*bottom*) the S-star HV 11223. Note the general similarity of the spectra. Both the TiO band and the Ca I line have similar strengths in these two red giants.

The ^{12}CN lines were taken from the SCAN-CN line list of Jørgensen & Larsson (1990). The predicted wavelenths of these lines are not very accurate, the prime purpose of the line list being the inclusion in opacity tables for the computation of stellar atmospheres. Therefore in some regions of interest, and when the lines could be found in the compilation of Davis & Phillips (1963), the wavelengths were adjusted.

For atomic lines, the primary source was the Kurucz & Peytreman (1975) and the Kurucz (1989) line lists. As a start, the *gf*-values of lines of interest were taken, when available, from Fuhr, Martin, & Wiese (1988) and/or from solar *gf*-values derived using MOOG (Sneden 1973), the Holweger-Müller (1974) solar model and the Kurucz solar flux atlas (Kurucz et al. 1984).

For synthesis of the first-overtone vibration-rotation bands of CO, we used the molecular constants of Dale et al. (1979) with *gf*-values from Chackerian & Tipping (1983). All lines with $0 \leq J \leq 120$ in the bands 2–0 to 12–10 were included in our syntheses.

The whole machinery was tested on some Galactic stars (δ Vir, HR 8714, HR 5590, HD 35155, and Aldebaran). Some *gf*-values were adjusted so as to yield solar mean abundances for Aldebaran in the 7390–7590 Å region, used for metal abundance measurements through lines of Fe I, Ni I, Co I, Cr I, Zr I, and Nd II. Many lines appeared too blended and were discarded. We were left with a set of useful Fe I, Ni I, Zr I, Nd II, Co I, and Cr I lines around 7500 Å (see Table 2), in addition to the 6707 Å Li I, the 8126 Å Li I, the 7699 Å K I, and the 7800 Å Rb I lines. For δ Vir we find good agreement with the abundance determination of Smith & Lambert (1985), e.g., [Fe/H] = +0.10 here versus +0.06 previously and [Ni/H] = +0.12 here and +0.11 previously. Finally, the Fe I, Ni I, Co I, and Cr I lines, with their adopted "Aldebaran" *gf*-values, were used together with equivalent widths measured in the Kurucz solar flux atlas (Kurucz et al. 1984) to derive abundances using the solar model of Holweger & Müller (1974). We find $\log \epsilon(\mathrm{Fe}) = 7.67 \pm 0.18$, $\log \epsilon(\mathrm{Ni}) = 6.40 \pm 0.14$, $\log \epsilon(\mathrm{Cr}) = 5.47 \pm 0.28$, and $\log \epsilon(\mathrm{Co}) = 4.92 \pm 0.43$, which, within the errors, compares well with 7.48, 6.25, 5.67, and 4.92 (Anders & Grevesse 1989; Holweger, Heise, & Kock 1990).

3.2. *Stellar Parameters*

The stellar parameters were derived from the photometry of WBF (see also Smith & Lambert 1989), who obtain bolometric luminosities by applying a bolometric correction, BC_K, to the mean value of M_K for each star. We note that we got very similar values by using a theoretical $(BC_V) - (V-K)$ relation based on the model atmospheres. The stars were assumed to be fundamental pulsators (Wood 1990) and $T_{\rm eff}$'s were derived using the $T_{\rm eff} - (J-K)$ from § 5 in WBF, based on the Ridgway et al. (1980) temperature scale. The $M_{\rm bol}$–period diagram in Figure 7 of WBF yields then masses from which we derive surface gravities. The

TABLE 2

ATOMIC LINE LIST FOR THE 7500 Å WINDOW

Species	λ (Å)	χ (eV)	log *gf*
Cr I	7400.226	2.90	−0.111
	7462.364	2.91	−0.183
Fe I	7401.690	4.19	−1.893
	7411.146	4.28	−0.602
	7440.921	4.91	−0.636
	7443.019	4.19	−1.900
	7445.767	4.26	−0.319
	7447.430	4.96	−0.983
	7461.531	2.56	−3.428
	7481.740	2.76	−4.280
	7481.930	4.80	−1.580
	7498.560	4.14	−2.089
	7511.036	4.18	−0.270
	7531.117	4.37	−0.572
	7540.439	2.73	−4.251
	7568.917	4.28	−1.210
	7583.797	3.02	−2.308
	7585.990	4.31	−0.513
Co I	7437.138	1.96	−3.341
	7553.963	3.95	−0.110
Ni I	7393.630	3.61	−0.631
	7414.510	1.99	−2.270
	7422.300	3.64	−0.460
	7525.140	3.64	−0.636
	7555.598	3.85	−0.357
	7574.080	3.83	−0.695
Zr I	7439.890	0.54	−1.879
	7553.000	0.51	−2.710
	7554.730	0.51	−2.232
Nd II	7513.770	0.92	−1.520
	7538.260	1.44	−0.860
	7540.970	1.14	−1.310
	7547.000	0.74	−1.660
	7577.540	0.20	−2.600

TABLE 3

ADOPTED STELLAR PARAMETERS

Star	M_{bol}[a]	T_{eff}	log g	$M/M_\odot$	ξ_{turb}
HV 11223	−6.19	3500	0.00	7	2.5
HV 1963	−6.76	3350	−0.27	7	2.0
HV 11366	−6.30	3450	0.00	7	2.0
HV 12179	−6.51	3400	0.00	7	2.5
HV 11329	−6.52	3600	−0.05	7	3.0
HV 1375	−6.24	3300	−0.30	7	3.0
HV 11452	−6.61	3400	−0.33	5	2.5
N371:C12	−7.83	3650	−0.20	15	2.5

[a] From Wood, Bessell, & Fox 1983.

masses are all around 5–7 $M_\odot$, as our sample stars lie around the tip of the AGB. The only exception is N371:C12 which, as a supergiant, was assigned a 15 $M_\odot$ mass. The masses are crude estimates, based on period-luminosity-radius relations from theoretical models.

We quickly discovered that we could not get good fits to the observed spectra for some of the stars with these parameters (see § 4). The T_{eff}'s were changed until a satisfactory fit was obtained for the 6700, 7500, 7700, and 8126 Å regions. This difference between the photometrically derived T_{eff} and the finally adopted spectroscopic T_{eff} (comprised between −390 and +260 K) may be explained by the strong variability of these AGB stars and by the uncertainties in the photometry and in the various calibrations used for such stars.

The metallicity adopted in the construction of the models was assumed to be [Z/H] = −0.6 on the logarithmic scale where 0.0 is solar; see Russell & Bessell (1989) and Spite, & Spite (1991) (for more comments on this choice see § 4.2.3). All abundances were scaled from the Anders & Grevesse (1989) solar mixture with the exception of Fe, taken from Holweger et al. (1990), and of N and O which were taken such as [N/H] = −0.2 and [O/H] = −0.8—see Luck & Lambert (1992)—and C which was chosen as follows. Different test models and spectral synthesis were run with C/O = 0.5, 0.8, and 0.9. The effect of the highest C/O ratios is to lower the TiO veiling and also, as a consequence, cool down the outer atmospheric layers, with the effect that the 7699 Å K I line is dramatically strengthened. Since we see no such strengthening in our observed spectra, we suppose that C/O < 0.8. Abundances derived from models for HV 1963 with C/O between 0.15 and 0.75 show little differences. For example, the Li abundance extracted from the 6707 Å line goes up by +0.3 dex and the K abundance by +0.2 dex when the C/O ratio drops from 0.5 to 0.15. This is of the order of, or smaller than, the other uncertainties. We thus decided to use C/O = 0.5, which translates to [C/H] = −0.73, for all the models. Note that the five stars for which we measured the C abundance have [C/H] $\lesssim$ −0.7.

The adopted parameters are shown in Table 3 and discussed further in § 4.2.

4. ABUNDANCE DETERMINATIONS

4.1. *General Outline*

Our abundance measurements are based on lines in 6 spectral regions. In Figure 2, we illustrate the different parts of the spectrum used in our analysis. The 6665–6735 Å region contains the Li I λ6707 resonance line. This part of the spectrum is heavily blanketed by TiO [especially γ(1–0) and γ(2–1)], as can be seen on Figure 2. We therefore also use the subordinate 8126 Å Li I line which is much less subject to molecular veiling by TiO and CN (see Fig. 2). We use the K I resonance line at 7699 Å as a control line in the measurement of the Li abundance. This part of the spectrum suffers from moderate blanketing by TiO. The TiO veiling around the Rb I line at 7800 Å is similar to that around the K I line. All the iron group element and *s*-process element lines used in this study are in the 7400–7600 Å region which is the least blanketed of all. At the lowest effective temperatures, veiling by TiO, VO, and LaO becomes more important. The CO bands lie around 2.2 μm where no other strong absorption features are present.

We generated models and synthetic spectra for four spectral regions (6700, 7500, 7700, and 8100 Å) using the first estimate for the stellar parameters. The continuum level was not set a priori in the observed spectra but the spectra were scaled in intensity to match the computed ones. Except for the stellar parameters (T_{eff}, log g, M) and, of course, the elemental abundances, the other parameters were the microturbulence, ξ_{turb}, and the FWHM of the Gaussian profile by which the synthetic spectra were convolved. This convolution accounts for the instrumental profile and the large-scale motions in the stellar atmosphere (macroturbulence, systematic velocity fields, rotation ...).

The spectra were compared in intervals of the order of 100 Å, which allowed us to assess "large-scale" characteristics of the spectra, especially the relative strength of TiO band heads. These provide additional constraints that would be overlooked by a very localized fitting around the spectral lines of interest. The average veiling (the depth of the TiO band-heads) is well modeled (see Fig. 2 as an illustration). Comparison of synthetic and observed spectra suggests that the amplitude of the wiggles are larger in the former. We suspect that this difference is due in part to the restriction of the TiO line list to ^{48}TiO lines. To test this suspicion, we computed a restricted line list for the γ system of TiO around the ~6707 Li I line for all five isotopes of Ti from ^{46}Ti to ^{50}Ti. A synthesis for the star HV 1963 shows that including all isotopes improves the match between calculated and observed spectra, but this is not likely to change our abundances by a large amount. We did not need to use any fudge opacity as Luck & Lambert (1982) did in their analysis of the 6707 Å Li I line region in M giants and supergiants. They could only get a good fit to the TiO spectral features at the expense of very low Al abundance (from the 6696 and 6699 Å lines). A more realistic Al abundance could be obtained by adding some extra quasi-continuous opacity in their synthetic spectra. They ascribed this "missing" opacity to a haze of faint

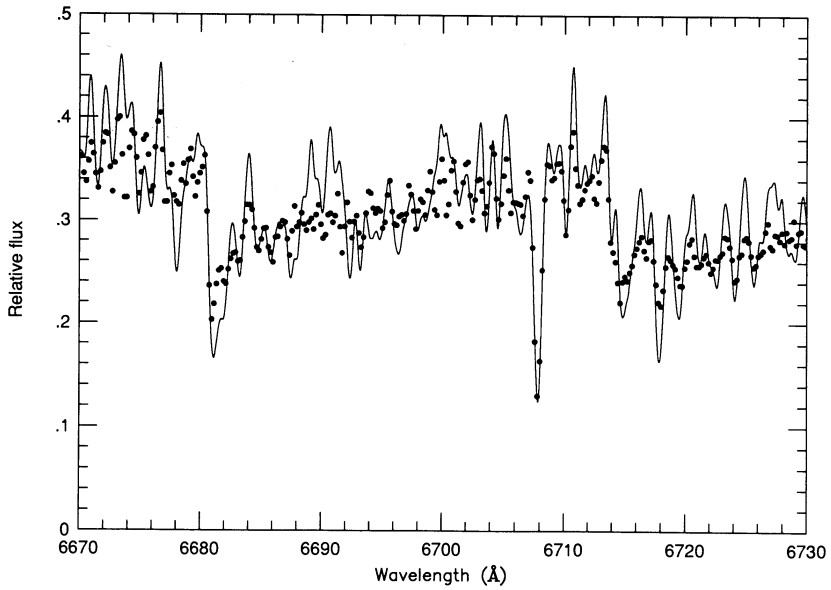

FIG. 2*a*

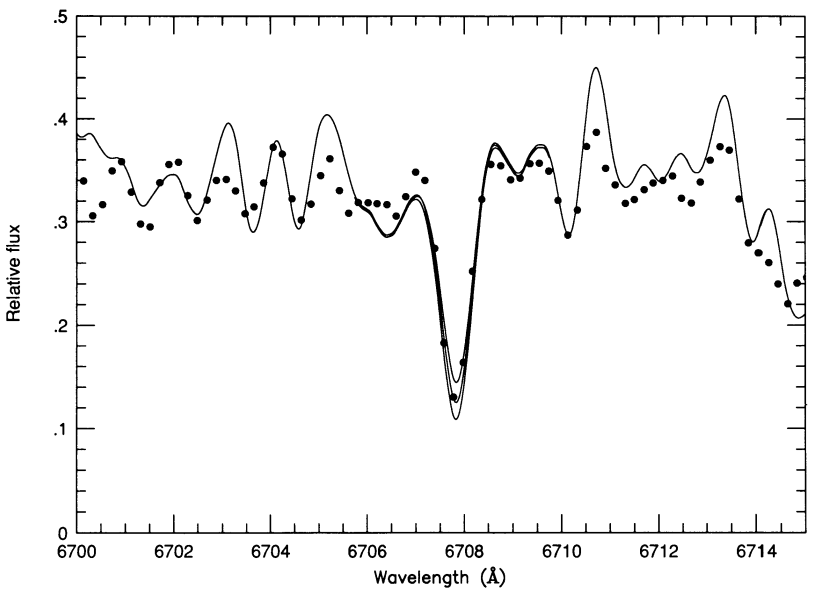

FIG. 2*b*

FIG. 2.—(*a–e*) Calculated and observed spectra for the star HV 1963. Abundances and other parameters have their final value (see tables). In the case of Li and K, calculated spectra for abundances of +0.5 and −0.5 dex from the central values are also shown. The feature at 8122 Å is terrestrial. The model continuum is at 1.0.

TiO lines and modeled it as a giant TiO line. We did not encounter such a problem when modeling Galactic giants (the Al lines are too faint to show in our SMC spectra). Our work demonstrates that combining good model atmospheres with extensive line lists allows the calculation of good synthetic spectra for cool stars.

Synthetic spectra for each star were generated for several plausible models. Through comparison of synthetic and observed spectra, the stellar parameters were further constrained and new spectra computed for various abundances of the chemical elements of interest. The quality of the fits was judged by eye, with emphasis on the lines' (or rather blends!) widths and depths, and large-scale characteristics like the TiO band features.

A constraint in the fitting procedure was that the potassium abundance derived from the 7699 Å K I line should be [K/Z] = 0.0 with the assumed [Z/H] = −0.6. This is justified by the fact that K is believed to be neither produced nor destroyed in any large amount and should largely follow the iron peak elemental abundances. There are no measurements of the K abundance in the SMC from F-type supergiants. Observations of Galactic stars suggest [K/Fe] ≈ 0 for [Fe/H] ≈ −0.5 (Gratton & Sneden 1987). Small (<0.5 dex and mostly much below that level) discrepancies were allowed, especially when fits to other parts of the spectrum

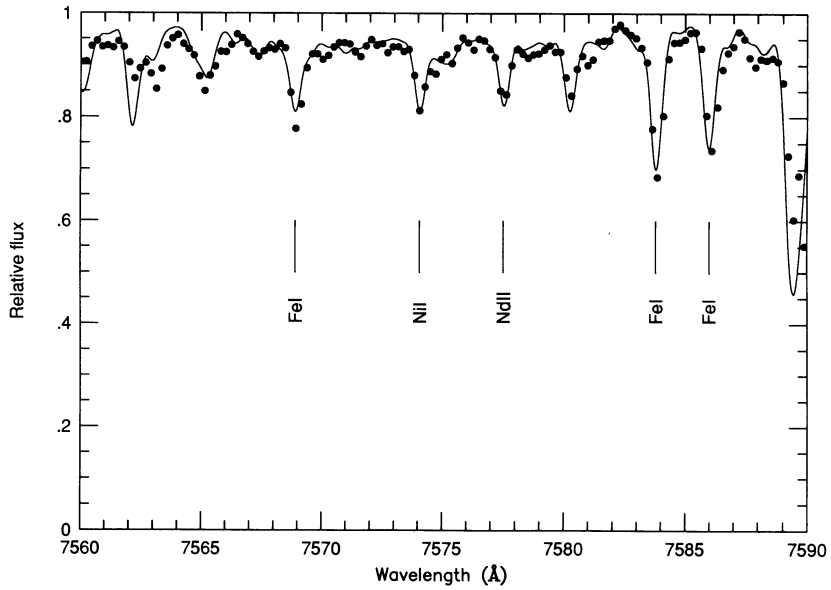

FIG. 2c

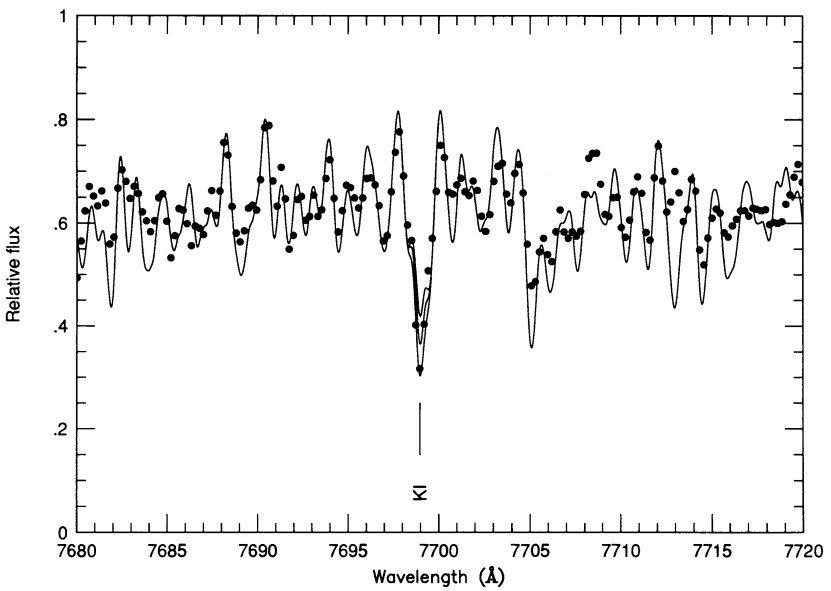

FIG. 2d

indicated a set of parameters that would not allow strictly [K/Z] = 0.0. We note that the uncertainties in most abundances we measure are of this order of magnitude, and there may, of course, be star-to-star variations of the metallicity.

4.2. *Atmospheric Parameters*

4.2.1. $T_{\rm eff}$

For a given spectral region the set of parameters giving a good match of the observed and synthetic spectra is not unique. For the 6707 Å Li I region one may, for example, offset a decrease of $T_{\rm eff}$ (which increases the strength of TiO veiling, and of the Li I line) with an increase of the C/O ratio (which will decrease the TiO veiling and increase the Li I line strength). One obtains a good fit in both cases but different abundances for Li. These two sets of parameters are, however, unacceptable for the K I line region, as the TiO veiling in the Li I and K I is of different intensity. The K I line becomes much stronger for the model of lower $T_{\rm eff}$ and higher C/O ratio, yielding an unacceptably low K abundance. The "pseudo-continuum" region between 7400 and 7600 Å is also sensitive to $T_{\rm eff}$ in our range of temperature ($\lesssim$3500 K). This permits the determination of $T_{\rm eff}$ by simultaneous fitting of the three (or four, including the 8126 Å) regions.

The effect of varying $T_{\rm eff}$ on the Li, K, and metal abundances is illustrated in Figure 3 for the star HV 1963. The K I and the Li I resonance lines behave very similarly, whereas the 8126 Å Li I line varies in the opposite sense (and very little, due to the much

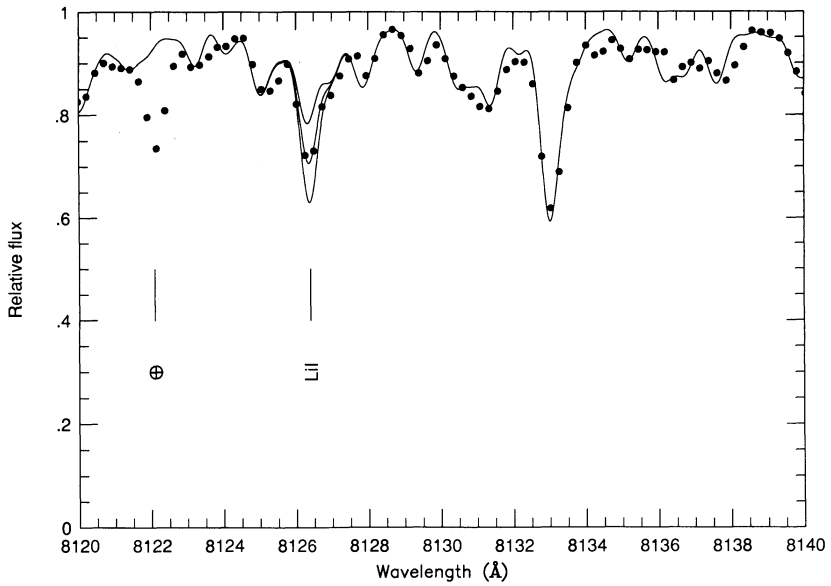

FIG. 2e

weaker molecular veiling in this region). Due to the differential sensitivity of the different spectral regions to temperature, the $T_{\rm eff}$ could be constrained to a 100 K uncertainty, largest for the coolest stars. Adopted values, ranging from 3300 to 3650 K, are listed in Table 3.

4.2.2. *Microturbulence*

The microturbulence parameter, $\xi_{\rm turb}$, was derived by essentially requiring the K/Fe abundance ratio to be solar. Figure 4 illustrates the variation of K, Li, and some metal abundances with $\xi_{\rm turb}$. We note the similarity of behavior of the K I and Li I λ6707 resonance lines with respect to $\xi_{\rm turb}$ changes which justifies our choice of the K I line as a control line. The inspection of other spectral regions sometimes invited us to small revisions of the microturbulence (≈ 0.5 km s^{-1}) in order to improve the fit (see also § 4.6). We note the low values we get for $\xi_{\rm turb}$ (≤ 3.0 km s^{-1}), which are slightly larger than typical values for late-type giants. This is expected for higher luminosity stars usually have higher microturbulences.

4.2.3. TiO *Veiling*

To derive abundances in the 7500 Å region, synthetic spectra were generated with abundances of the species of interest varied by 0.5 dex steps. The best fit was then estimated by eye. The Ti abundance was not varied when fitting the atomic lines, as the effect of its varying is to shift the whole spectrum up and down, without changing much the atomic line/TiO "continuum" ratio. As a result we do not derive Ti abundances.

The sensitivity of the local "pseudo-continuum" level (set by the molecular veiling) to the variation of some parameters (e.g., C/O ratio, Ti abundance) in the modeling complicates the fitting process. The accuracy of the derived abundances will not be much affected and the fitting process considerably simplified if these parameters are set to a reasonable value and not varied.

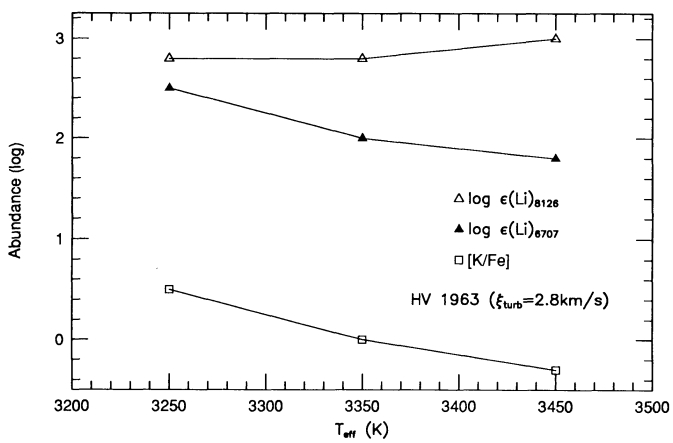

FIG. 3.—Illustration of the effect of varying $T_{\rm eff}$ of the model on the Li and K abundances for the star HV 1963. Note the similar behaviour of the 6707Å Li I and the K I resonance lines. The abundance scale is logarithmic, with log ϵ(H) = 12 for Li, and relative to the solar value for [K/Fe].

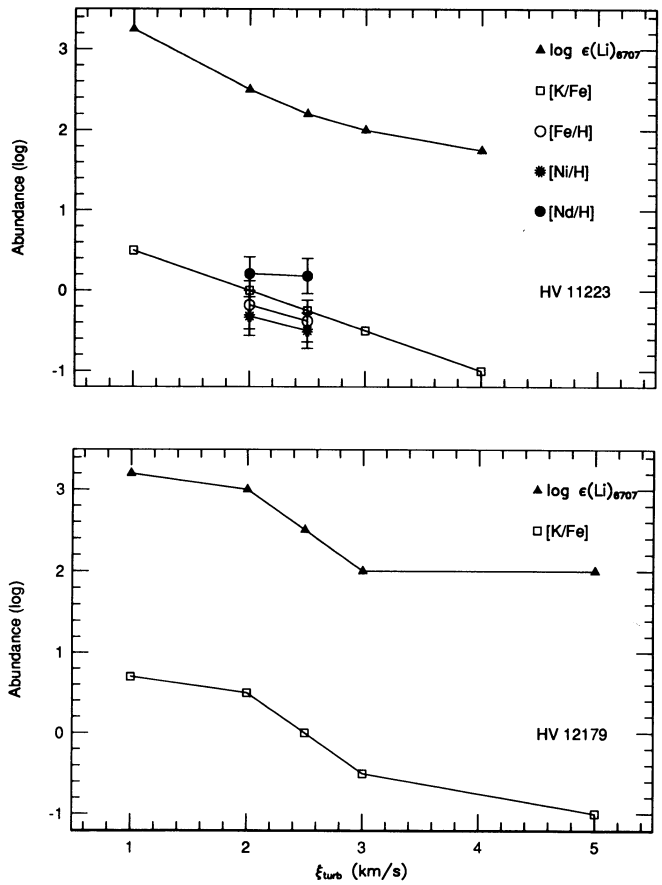

FIG. 4.—Effect of varying the microturbulence on the abundance of various species for the stars HV 11223 (*top*) and HV 12179 (*bottom*). Note again the similar behaviour of the Li I and K I resonance lines. Abundance scale as in Fig. 3.

When C or Ti abundance is varied, one ought to recompute a model with the new abundances and iterate, as these abundances affect the atmospheric structure. An increased Ti abundance, for example, leads to a model with hotter outer layers and thus the lines formed in these layers (like the strong TiO lines themselves, and the resonance lines of Li I and K I) weaken. The higher Ti abundance is partially compensated for by a decrease of the TiO lines strength, due to the increased temperature of the outer layers. Tests on δ Vir show that the abundance of Li derived from the 6707 Å line varies by at most 0.1 dex when the Ti abundance changes by 0.2 dex in the model. A change of the overall metallicity of the model by 0.4 dex has approximately the same effect. The K abundance from the 7699 Å line varies in a similar way. Greater changes arise when changing $T_{\rm eff}$ and, for the atomic lines, $\xi_{\rm turb}$. Thus the metallicity was kept [Z/H] = −0.6 in the models and the Ti abundance was assumed to be [Ti/H] = −0.6, which a posteriori appears to be a good approximation given the metallicity derived from Fe I and Ni I lines (and also Co I and Cr I) (see Table 5 and § 5.1). As already pointed out, the C/O ratio was kept equal to 0.5 in all the models.

4.2.4. *Additional Remarks*

It should be emphasized that due to the interplay of all the parameters ($T_{\rm eff}$, abundances, $\xi_{\rm turb}$, ...) the convergence toward final abundances requires some careful exploration of the parameter space. Some lines used are strong, often saturated. This leads to large uncertainties in the abundances and to sensitivity to microturbulence. The 6707 Å Li I resonance line is sometimes very saturated and thus its strength depends on various conditions at the very top of the atmosphere. However, the use of the 7699 Å K I resonance line, formed in similar layers and conditions, as a control line may remove most of the uncertainty due to that problem.

Finally, a word on non-LTE effects and dynamics. LPVs atmospheres are not static. They are pulsating and shock waves crossing the photosphere may give rise to large amounts of ionizing radiation. Systematic velocity fields will distort the profiles of some lines (we seem to be seeing that for HV 11366 and HV 11223 for Li I) and may explain the smooth aspect of the TiO veiling in HV 1375. Scholz (1992) has discussed the effect of velocity gradients and discontinuities in LPVs atmospheres on the emergent spectra, calculating curves of growth for a few typical lines. The differences in abundances may be large but are greatly reduced if microturbulence is present in the atmosphere. However, it appears impossible to model satisfactorily the outflow/infall velocities with a single microturbulence velocity for all the lines. That may explain some of our problems when modeling the CO lines, which seem to demand a lower microturbulence than some other lines (like TiO).

We note the different Li abundances we derive from the two Li I lines (6707 Å: $\chi_{\rm exc}$ = 0.0 eV, and 8126 Å: $\chi_{\rm exc}$ = 1.85 eV and originating from the upper level of the former transition). The abundance from the 8126 Å line is systematically higher (from 0.0 to

TABLE 4

MEASURED STELLAR ABUNDANCES

STAR	[Fe/H]	[Ni/H]	[Co/H]	[Cr/H]	[Zr/H]	[Nd/H]	log ϵ(Li) 6707 Å	log ϵ(Li) 8126 Å	$^{12}C/^{13}C$	[C/H][a]
HV 11223	−0.38	−0.50	−0.45	−0.40	−0.23	+0.18	+2.5	+3.2	9	−0.73
HV 1963	−0.43	−0.53	−0.47	−0.10	−0.65	+0.20	+2.5	+3.0	7	−1.26
HV 11366	−0.42	−0.52	−0.18	0.00	−0.30	+0.45	+1.3	+2.5	[b]	[b]
HV 12179	−0.34	−0.66	0.00	−0.60	−0.35	+0.51	+2.5	+3.0	5	−1.76
HV 11329	−0.37	−0.36	−0.85	−0.57	−0.63	+0.03	+3.5	+3.5	[b]	[b]
HV 1375[c]	−0.65	−0.73	...	−0.85	−0.35	−0.03	+3.0	+3.0	[b]	[b]
HV 11452[c]	−1.04	−0.35	...	−0.85?	−0.30	−0.10	+3.0	...[b]	5	−0.96
N371:C12	−0.35	−0.39	...	−0.60?	−0.60?	−0.35	−0.8	...[d]	25	−1.06

NOTE.—For the species where a sufficient number of lines could be analyzed (Fe I, Ni I and often Nd II), the standard deviations range mostly between 0.2 and 0.3. For individual lines (including the Li I lines) the uncertainty lies around 0.5 dex. The situation is better for the weaker and less blanketed 8126 Å Li I line. For C abundances, the error we derive from comparing various synthetic spectra is about ±0.3 dex (the error may be smaller for HV 11223). The uncertainty in the $^{12}C/^{13}C$ ratio is about ±3 for all stars but N371:C12 for which it is about ±7. See text.

[a] May not be very reliable, see text.
[b] No observation.
[c] Most uncertain measurements.
[d] Not detected.

an extreme 1.2 dex for HV 11366). The model atmosphere used in the analysis of the 8126 Å line (and CO bands) is derived from spectra obtained at a different time. Since LPV atmospheres are variable structures, use of a single model may lead to systematic differences between the different regions. One may also expect non-LTE effects to occur, like overionization and overexcitation of Li. Use of LTE is then likely to underestimate the Li abundance, with a larger error applying to the resonance line. We prefer not to venture into trying the hazardous art of predicting non-LTE effects, especially in variable stars.

4.3. *Effects of Sphericity*

We shall discuss the importance of the choice of the stellar mass for the derived Li (and K) abundance in the special case of HV 1963. We recall that the final adopted model for this star is $T_{\rm eff} = 3350$ K, $\log g = -0.27$, $M = 7\,M_\odot$ and $\xi_{\rm turb} = 2.0$ km s^{-1}. As we know the luminosity of this object, choosing a lower mass, e.g., $3\,M_\odot$, would force us to adjust $\log g$ to −0.66. We computed such a model, and we derived about the same Li and K abundances as with the $M = 7\,M_\odot$ model.

We also computed the corresponding plane-parallel (PP) models. The PP $\log g = -0.27$ model yields a Li abundance lower by −0.25 dex and a K abundance lower by −0.15 dex. The $\log g = 0.66$ PP model yields abundances lower by −0.4 and −0.3, respectively. The fits are of good quality in both cases. The difference between the Li abundances derived with the PP models of different surface gravity (difference we did not find in the spherical case) is due to the difference in gravity which, when decreased, leads to a decrease of the TiO veiling and a smaller decrease of the Li line strength. As a result lower Li abundance is necessary to account for the Li line/TiO "pseudo continuum" contrast. We note that, in comparison, changing $\xi_{\rm turb}$ from 2.8 to 2.0 km s^{-1} induces changes of +0.25 dex for the Li abundance and +0.5 dex for the K abundance.

We found the same K and Li abundances from the two spherical models of different gravity (although with a worse fit for the lower mass model). We explain the absence of differences in the derived abundances by a fortuitous cancellation of gravity and sphericity effects. A lowering of gravity would induce, as in the plane-parallel case, a lowering of the TiO veiling and thus of the measured Li abundance. But at the same time atmospheric extension increases and the temperature of the outer layers drops, which

TABLE 5

SUMMARY OF MEASURED ABUNDANCES

Star	[z/H][a]	[Zr/z]	[Nd/z]	[s/z][b]	log ϵ(Li)[c]	$^{12}C/^{13}C$	[Rb/z][d]
HV 11223	−0.44	+0.21	+0.62	+0.42	+2.85	9	−0.5??
HV 1963	−0.48	−0.17	+0.68	+0.26	+2.75	7	≤−1.0
HV 11366	−0.47	+0.17	+0.92	+0.55	+1.90	...	−1.0
HV 12179	−0.50	+0.15	+1.01	+0.58	+2.75	5	−0.5??
HV 11329	−0.37	−0.26	+0.40	+0.07	+3.50	...	−0.9
HV 1375	−0.69	+0.34	+0.66	+0.50	+3.00	...	≤−1.0
HV 11452	−0.70	+0.40	+0.60	+0.50	+3.0	5	≤−1.2
Average	−0.52	+0.12	+0.70	+0.41	+2.82	6.5	≤−0.9
σ	0.13	0.25	0.21	0.18	0.48	1.9	≥0.25
N371:C12	−0.37	−0.23?	+0.02	−0.11	−0.8	25	−1.3[e]
Average −C12	−0.15	+0.35	+0.70	+0.52	+3.62		≤0.4?

[a] z is the average of the Fe and Ni abundances.
[b] s is the average of the Nd and Zr abundances.
[c] Straight average of the 6707 Å and 8126 Å abundances.
[d] Relative to solar photospheric value: $\log \epsilon(\mathrm{Rb}) = 2.60$.
[e] From AAT spectrum.

has the opposite effect of increasing the TiO veiling. (Note: The extension defined as $d = (R_{\tau_{Ross}=10^{-5}}/R_{\tau_{Ross}=1}) - 1$, where $R_{\tau_{Ross}=x}$ is the radius at which the Rosseland optical depth is x-, is $d = 0.07$ for the $M = 7\ M_\odot$ and $d = 0.19$ for the $M = 3\ M_\odot$ model.) As a result, the veiling of the lower gravity spherical model is larger than in the higher gravity spherical model. The opposite is true of the PP models. Thus, sphericity effects counterbalance here the effect of decreased gravity, and the abundance differences are minimal.

As a final remark, one may note that from our experience, it is important to use well-blanketed models and extensive line lists, and high-resolution spectra (for, e.g., a good determination of the line profiles, ξ_{turb}). The introduction of spherical symmetry certainly adds to the accuracy of the measured abundances, especially for very low gravity, low-mass stars, but the differences between PP and spherical models are often smaller than the other uncertainties (see also Plez 1990). This is in accordance with Jørgensen's (1992) affirmation in his paper on sampling methods that "a correct sampling of water opacity has been of greater importance to the model structure of M stars than the combined effect of all the other improvements (...) during the last 25 years!"

4.4. *Abundances and Uncertainties*

The abundances derived for Li, Fe, Ni, Nd, Zr, (and Cr, Co), Rb, C, and $^{12}C/^{13}C$ are displayed in Tables 4 and 5. We shall add some remarks on the quoted values and their uncertainties. The quoted errors reflect mostly the uncertainties in the match of observed and calculated spectra: up to ± 0.5 dex, depending on the star and the spectral lines, being largest in the coolest stars and in the most blanketed spectral regions. The Li abundance derived from the 8126 Å line is more reliable in that respect than the abundance from the more saturated 6707 Å line. These are maximum errors. Some uncertainty in the fundamental parameters is taken into account in some cases, such as for the C abundances or when the stellar parameters seemed difficult to determine (HV 1375). The errors do not reflect possible non-LTE effects, dynamics of the atmospheres, errors in the model atmospheres or errors in the molecular line lists. We have seen that changes in mass (and thus log g) will not have a large impact (maybe at the level of the errors in the most unfavorable cases). Small changes in the microturbulence will induce larger changes in the abundances ($\approx \pm 0.5$ dex per km s^{-1}). For the metals, for each of which we had up to a dozen lines or more, we give the average abundance and the σ calculated from the determinations for all lines. For an individual line, the uncertainty is often of the order of ± 0.5 dex. For Li we give the two abundances from the two lines as well as the average. We decided to use a straight mean of the two determinations.

4.5. Rb *Abundances*

We attempted the measurement of Rb abundances from the 7800 Å resonance line. The molecular veiling is quite strong in this region, and, contrary to expectation, the Rb line is weak in the spectra, as shown in Figure 5. For most stars we find abundances [Rb/Fe] ≈ -1.0 (see Table 5). Decreasing further the Rb abundance to -1.5 or -2.0 in the calculated spectra does not change greatly the appearance of the line. Our abundances could be, and in some cases are, upper limits. As we are particularly interested in a possible difference in the Rb abundance between the M supergiant and the S stars, we used a higher resolution spectrum of N371:C12, taken at the AAT 4 m telescope, to try to derive a firmer value for the Rb abundance in this star. We get [Rb/Fe] $\approx -1.3 \pm 0.3$ [with a solar photospheric log ϵ(Rb) = 2.60 as a reference]. If the Rb line is blended with an unidentified feature, this becomes an upper limit. Non-LTE effects could arise, as the ionization potential of Rb is low (4.18 eV). These non-LTE effects should affect the Rb abundance in other M supergiants in a similar fashion. We took a spectrum of Betelgeuse to check this possibility. We derive [Rb/Fe] $= -0.6 \pm 0.2$ (actually: [Rb/Fe] ≈ -0.5 if [Fe/H] $= -0.3$ and [Rb/Fe] ≈ -0.7 if [Fe/H] = 0.0), using model atmosphere parameters suggested by Lambert et al. (1984): $T_{eff} = 3800$ K, log $g = 0.15$ and $M = 20\ M_\odot$. For

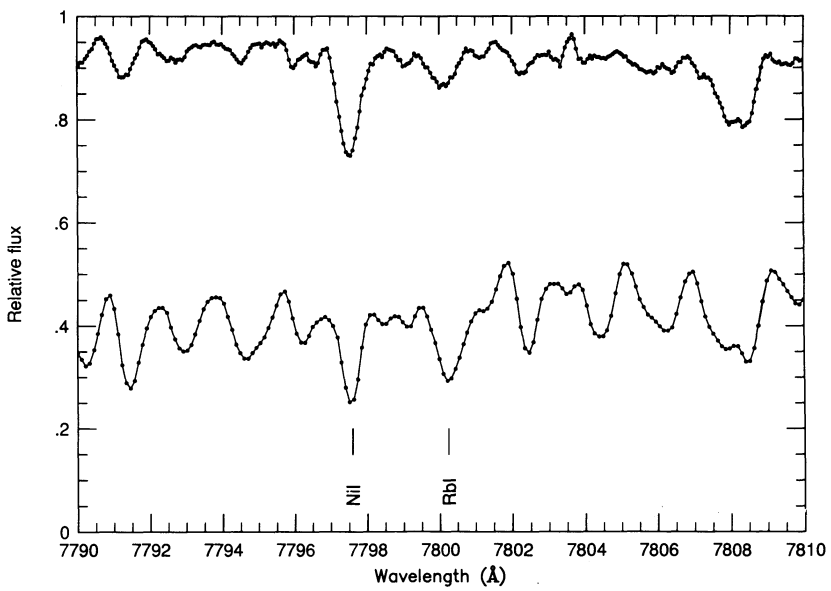

FIG. 5.—Observed spectra of N371:C12 (*upper*) and Betelgeuse (*lower*) in the Rb I spectral region. The lower spectrum has been shifted down by 0.5. Flux units arbitrary. Note the weakness of the Rb I line in N371:C12.

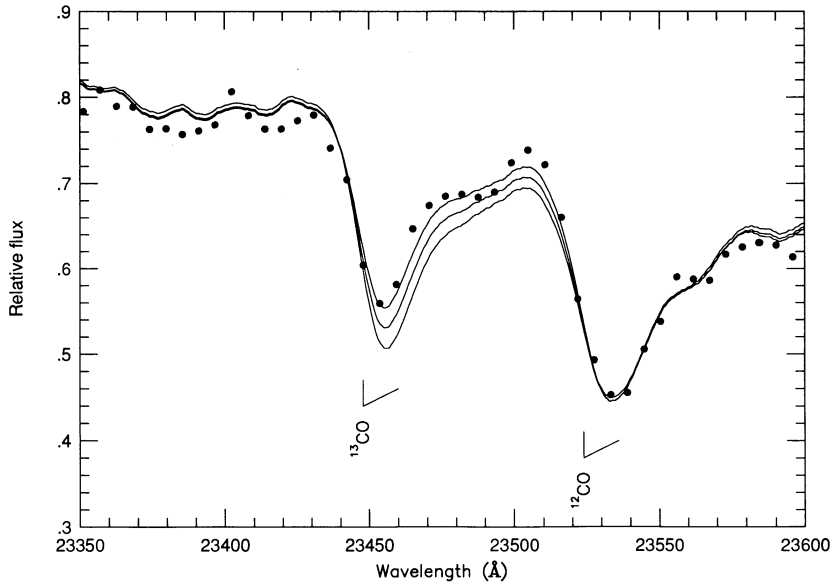

FIG. 6.—CO spectrum for the star HV 11223. Dots are the observation; three synthetic spectra are plotted for [C/H] = −0.73 and $^{12}C/^{13}C$ = 2, 5, and 10.

Aldebaran, we find -0.4 ± 0.1, in accordance with Lambert & Smith (1993). Inspection of a dozen spectra of Galactic M supergiants shows a Rb line stronger than in N371:C12, suggesting abundances similar to Betelgeuse. We conclude that non-LTE effects on Rb abundance are probably weak, and in any case not of the factor of ~10 needed to bring the Rb abundance in N371:C12 up to the Galactic M giants level. We note also that we use a resonance line of K I to determine the abundance of potassium, another alkali with a low-ionization potential. Although we force the K/Fe ratio to be about solar in our analysis, we would likely have noticed the presence of large non-LTE effects. The fact that we do not see any peculiar behavior of the K I line reinforces our conviction that non-LTE effects are probably small.

4.6. CO *and the* C *Abundances*

Our C abundances determinations are hampered by the poor resolution and low signal-to-noise ratio of our observations in the 2.2 μm spectral region. We tried to assess a "best value" based on fits of the ^{12}CO (2–0) and of the ^{12}CO (4–2) and ^{13}CO (2–0) band heads and further across the less saturated parts of the bands (Fig. 6). These fits usually gave two or three different C abundances depending on where the fit was forced. The uncertainties reflect this situation. The $^{12}C/^{13}C$ should be more reliable, as the quoted values were derived after examining a variety of fits for different $^{12}C/^{13}C$ and different C abundances. The $^{12}C/^{13}C$ is slightly dependent upon the C abundance and the errors quoted reflect the uncertainties in both the fitting and the C abundances. We should add that the CO spectra constrained the choice of ξ_{turb} toward lower values, as the calculated absorption features [the unresolved band heads of the ^{12}CO (2–0) and (4–2) bands and the ^{13}CO (2–0) bands] tend to become very strong and yield very low C abundances, at the high end of the ξ_{turb} range.

5. DISCUSSION

5.1. *Metallicity*

Recent abundance determinations from high-resolution spectroscopy are available for SMC F-type supergiants (Spite, Spite, & François 1989; SSF; Russell & Bessell 1989; RB) and SMC Cepheids (Luck & Lambert 1992; LL): a comparison with abundances derived here from luminous red giants is instructive. Reviews of the composition of the SMC are provided by Russell & Dopita (1992) and Russell (1993). We note that the red giants studied here are rather massive ($M > 5\,M_\odot$) and, hence, young (recall that the total lifetime of a 5 $M_\odot$ star is less than 10^8 yr). The stars from SSF, RB, and LL quite probably overlap in mass with the red giants studied here and a comparison of the various abundance determinations provides a simple check on our abundances derived from rather complex spectra.

In making this comparison for iron-group elements, we assume, as calculations of TP-AGB stars suggest, that the surface abundances of these elements are unaffected by the dredge-up of material from the He-burning shell. The abundances would be affected if either the mass fraction of the iron-group elements were reduced or the He/H ratio at the surface were increased through the dredge-up. With the possible exception of HV 1375 and HV 11452, the [Fe/H] of the S stars are identical to within the errors of measurement, suggesting that the iron-group abundances are unaltered by the dredge-up. Therefore, we use abundances from the S stars in the comparisons with the F-type supergiants and the Cepheids. (Note the dredge-up could add material deficient in iron but rich in helium to the atmospheres and an analysis of such an atmosphere, which assumes a normal He/H ratio, might return a quasi-normal iron abundance because the iron deficiency is compensated for by the reduced opacity of the He-rich material.)

Our best-determined single abundance is Fe for which up to 16 lines of Fe I are used. An average of all Fe abundances results in [Fe/H] = -0.50 ± 0.24. HV 11452 has a much lower Fe abundance than the rest of the sample; however, as discussed earlier, this

TABLE 6

AVERAGE ABUNDANCES IN THE SMC

Element	PSL[a]	LL[b]	SSF[c]	RB[d]
[Fe/H]	-0.50 ± 0.24	-0.51 ± 0.10	-0.66 ± 0.10	-0.65 ± 0.17
[Ni/H]	-0.50 ± 0.14	-0.45 ± 0.27	-0.41 ± 0.15	-0.33 ± 0.24
[Cr/H]	-0.50 ± 0.31	-0.33 ± 0.06	-0.65 ± 0.11	-0.49 ± 0.25
[Z/H]	-0.50	-0.47	-0.58	-0.54

[a] This Paper.
[b] Luck & Lambert 1992.
[c] Spite, Spite, & François 1989.
[d] Russell & Bessell 1989.

star's spectrum was difficult to fit and if it is excluded then [Fe/H] = -0.42 ± 0.11. The other well-determined abundances are Ni and, to a lesser degree, Cr and Co. In Table 6 we present a comparison of our average abundances with the averages from LL, SSF, and RB. The overall agreement from the four studies is excellent: a mean Fe abundance from all four groups is [Fe/H] = -0.59 ± 0.08. There is no hint of systematic differences in either [Ni/Fe] or [Cr/Fe] abundances and these three elements can be combined to provide an estimate of the mean metallicity of the young stars of the SMC. As Fe is usually the "best determined" of the abundances (the most lines) we assign [Fe/H] from each study a weight of 4, [Ni/H] a weight of 2 and [Cr/H] a weight of 1. We list these means as [Z/H] in Table 6: the averages from the four studies are in close agreement and a combination of all the values yields [Z/H] = -0.53 ± 0.04 as an estimate of the mean metallicity of the SMC field. The high-resolution studies also agree with the low-resolution (≈ 5 Å) spectroscopic abundances of Thévenin & Jasniewicz (1992), who find [Fe/H] = -0.46 for the SMC field.

There may be small systematic differences between the study here and the other three, as we derive abundances using Aldebaran as a standard star, whereas the other studies use Canopus as a standard. An inspection of the abundances reveals no significant trends, suggesting that there are no large inherent differences between the analyses of the F supergiants and the M supergiants, and that both Aldebaran and Canopus have a near solar metallicity.

A discussion and comparison of the heavy element abundances (usually thought of as the *s*-process elements) is more difficult due to far fewer and weaker lines. Also, seven of the stars analyzed here are probably TP-AGB stars which have altered their initial heavy element abundances via internal *s*-process nucleosynthesis and subsequent mixing. Our lone example of a core-burning supergiant is N371:C12. If we average the Fe and Ni abundances for this star we obtain [Z/H] = -0.37 which then leads to [Zr/Z] = -0.23 and [Nd/Z] = $+0.02$ for this star. Although these individual numbers for N371:C12 should not be given much weight, they appear to conform to an emerging abundance pattern in the SMC field in which the light neutron-capture species (such as Y and Zr) are underabundant relative to the heavy neutron-capture elements (such as Ba and La). The pattern was noted first by Russell & Bessell (1989). Straightforward averages for the SMC abundances reveal [Nd, Sm/Y] = $+0.33$ from LL, [Ba, La, Ce, Nd/Y, Zr] = $+0.40$ from SSF, and [Ba, La, Ce, Nd, Sm/Y, Zr] = $+0.20$ from RB. This same abundance pattern is found in the low-resolution work of Thévenin & Jasniewicz (1992) and is noted in the recent review by Russell (1993).

5.2. *Third Dredge-up: s-Processing*

AGB stars, including the present sample of S stars, are, through the third dredge-up, enriched in products of nucleosynthesis from the He-shell around the C-O core. These luminous S stars are expected to have experienced many thermal pulses and the subsequent dredge-up of carbon and *s*-processed products. Repeated dredge-up of carbon should convert the star to a carbon star. Since all the very luminous AGB stars in the Clouds are oxygen-rich S stars, it is supposed that sufficient carbon is burnt to nitrogen by operation of the H-burning CN-cycle at the hot base of the convective envelope; we discuss this phase of the H-burning in the next section. The abundance distribution of the *s*-process elements in the S stars is expected to have reached the asymptotic form achieved after ~ 10 or fewer thermal pulses (Busso et al. 1988).

5.2.1. Zr *and* Nd

The Zr/Nd ratio of the supergiant N371:C12 is slightly less than the solar ratio at [Zr/Nd] ≈ -0.23. Russell & Dopita give [Zr/Nd] ≈ -0.6 for the SMC field stars. To within the errors, N371:C12 is representative of the field stars.

Comparison of the *s*-process elements studied here (Zr and Nd) in the S stars shows the AGB stars to be *s*-process enriched (Table 5) relative to N371:C12 and also relative to the field F supergiants (see summary by Russell & Dopita 1992). The average enrichment of Zr and Nd at [*s*/Fe] $\approx +0.5$ is typical of the Galactic S stars (Lambert & Smith [1993]). As noted by Smith & Lambert (1989), WBF's identification of these stars from the presence of ZrO bands is confirmed by the elemental abundances.

Although the average enrichment of Zr and Nd is typical of that observed in Galactic S stars, the Zr/Nd abundance ratio is considerably lower than almost all local S stars and much lower than solar. As the observed ratio is a mixture of the original envelope composition and of the (presumably) highly processed *s*-process material, we use the precepts of Tomkin & Lambert (1983) to estimate the abundance ratio in the *s*-process material added by the thermal pulse. Following their work we derive:

$$\frac{N^s_{\rm Zr}}{N^s_{\rm Nd}} = \frac{\epsilon_\odot({\rm Zr})}{\epsilon_\odot({\rm Nd})} \frac{10^{[{\rm Zr/Fe}]_*} - 10^{[{\rm Zr/Fe}]_{\rm ref}}}{10^{[{\rm Nd/Fe}]_*} - 10^{[{\rm Nd/Fe}]_{\rm ref}}}, \quad (1)$$

where N^s_{Zr} and N^s_{Nd} are the abundances of Zr and Nd in the *s*-process enriched region, $\epsilon_\odot$(Zr) and $\epsilon_\odot$(Nd) are the solar abundances, and $[X/Fe]_*$ and $[X/Fe]_{ref}$ are the observed abundances of element X relative to Fe, in standard spectroscopic bracket notation, in the SMC S-stars (denoted by asterisk) and in a standard reference abundance pattern (i.e., N371:C12 or the field Supergiants). We have assumed (and that is certainly justified) that $f_s/f_e\, N^s_{Fe}/N^e_{Fe} \ll 1$, where f_s and f_e are the mass fraction of the dredged-up material and of the envelope respectively, and N^s_{Fe} and N^e_{Fe} are the Fe abundances in the dredged-up and the envelope material.

For the seven SMC stars, N^s_{Zr}/N^s_{Nd} varies between 1.1 and 8.1 (with N371:C12 as reference) with the average at 2.3. This ratio is 3.7 when the abundances tabulated by Russell & Dopita (1992) are used as reference. The ratios are even lower when only the five S-stars with the most reliable abundances are used.

This is *not* expected of a thermally pulsing star, for which an exponential distribution of neutron exposures will characterize the material added to the envelope (Ulrich 1973). For example, Malaney (1987a) predicts the Zr/Nd ratio to decline from 340 at $\tau_0 = 0.1$ through 15 at $\tau_0 = 0.4$ to 6 at $\tau_0 = 1.0$ mb^{-1}, where τ_0 is the mean neutron exposure for the exponential distribution of exposures, and $\tau_0 \approx 0.3$ characterizes the solar *s*-process abundances (Zr/Nd = 21). The fact that the initial abundances of the heavy elements, Ba-Nd, are slightly nonsolar in the SMC, seems unlikely to affect significantly the predicted Zr/Nd ratio. It may be possible to reduce the predicted Zr/Nd ratio by discarding the assumption of an exponential distribution of neutron exposures. A single severe exposure decreases the Zr/Nd ratio: Malaney (1987b) predicts Zr/Nd to decrease from 23 at $\tau = 1.0$ to 9 at $\tau = 1.1$ and 0.8 at $\tau = 1.5$ (see also § 5.2.2). Identification of the observed Zr/Nd ratio with material exposed just once to neutrons would involve discarding the idea that some of the *s*-processed material in the He-shell is exposed to neutrons again at the next thermal pulse. This reexposure seems to have adequate theoretical justification from models of thermally pulsing intermediate-mass AGB stars and was shown by Ulrich (1973) to result in an exponential distribution of exposures. The reexposure is described by an overlap factor (usually designated *r*) and $r = 0.25$ is typical (Busso et al. 1988). We are reluctant to suggest that the overlap factor is very much smaller than expected, but there are theoretical proposals suggesting that the energy release from the neutron source $^{13}C(\alpha, n)^{16}O$ at the top of the He-shell may split this region from the convective layers of the He-shell in which neutrons from primarily $^{22}Ne(\alpha, n)^{25}Mg$ may drive the *s*-processing (Sweigart 1974; Bazan & Lattanzio 1992). Provided that a high ^{13}C abundance is achieved at the top of the He-shell, the exposure to neutrons may reach the desired levels ($\tau \approx 1.3$ mb^{-1}). Presence of a hot-bottom envelope rich in ^{13}C may make it easier to achieve these levels. If subsequent dredge-up into the convective envelope is confined to the top of the He-shell, *s*-process enrichment at the surface will resemble that achieved in a single exposure to neutrons.

A low Zr/Nd ratio is not peculiar to the SMC S-stars, however, as not all *s*-process enriched stars in the Galaxy show a solar system *s*-process distribution. Luck & Bond (1991) suggested that the average ratio of light *s*-process to heavy *s*-process ([ls/hs]) abundances decreased with decreasing metallicity in the Barium and CH stars. This effect was demonstrated dramatically by Vanture (1992) for the metal-poor CH giants; the relation of [ls/hs] versus metallicity was reviewed by Smith (1993) for the barium and CH subgiants and giants. Qualitatively, such an decrease of [ls/hs], or an increase in the neutron exposure, with [Fe/H] is expected for an *s*-process neutron source which is independent of metallicity, as shown by Clayton (1988). In as much as the structure of a thermal pulse is independent of metallicity, the $^{13}C(\alpha, n)^{16}O$ neutron source is expected to satisfy the above criterion to a larger degree than the $^{22}Ne(\alpha, n)^{25}Mg$ neutron source.

In Figure 7 we plot the derived abundance ratio N^s_{Zr}/N^s_{Nd} versus [Fe/H] for Galactic S, Ba, and CH stars, as well as the SMC AGB stars, together with Malaney's (1987a, b) predictions. In this plot, the SMC stars do not stand out at all and have N^s_{Zr}/N^s_{Nd} ratios that are quite typical of Galactic stars at these metallicities. The simple interpretation of Figure 7 is that the neutron exposure

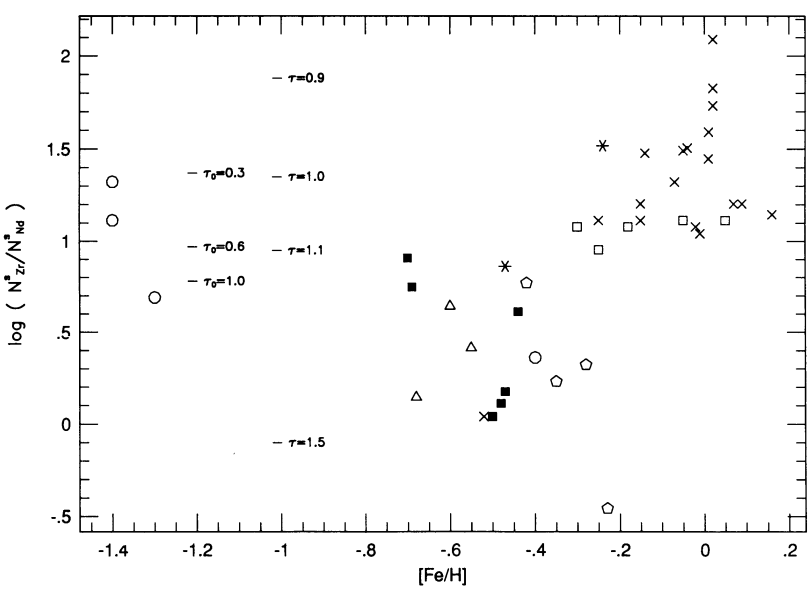

FIG. 7.—Zr/Nd ratio in the *s*-processed material versus metallicity, in various samples of stars. *Open squares*: Smith 1984, Ba stars. *Open circles*: Vanture (1992), CH stars. *Stars*: Tomkin & Lambert (1986), Ba stars. *Pentagons*: Kovacz (1985), Ba stars. *Open triangles*: Smith & Suntzeff (1987), Ba stars. *Crosses*: Smith & Lambert (1985, 1986, 1990b), S stars. *Filled squares*: this work. The Zr/Nd abundance ratios predicted by Malaney's model with an exponential distribution of neutron exposures (1987a) and single-exposure model (1987b) are marked with their respective τ_0 and τ exposures.

is increasing, i.e., Zr/Nd decreasing, as [Fe/H] decreases; this is predicted qualitatively, provided that $^{13}C(\alpha, n)^{16}O$ is the neutron source driving the *s*-process. Note, again, that at low metallicities ([Fe/H] $\lesssim -0.3$) there is an indication that single high neutron exposure models fit the data better than exponential distributions of neutron exposures. Similar conclusions were reached by Malaney (1987b) and Vanture (1992).

For the SMC S-stars, this result is somewhat surprising as these are all very luminous AGB stars with (presumably) large core-masses (see, however, Blöcker & Schönberner 1991, and Boothroyd & Sackmann 1992 on the breakdown of the core mass-luminosity relation at high luminosity) and are thus prime candidates for an *s*-process driven by the $^{22}Ne(\alpha, n)^{25}Mg$ neutron source.

We note that, in the SMC stars, the Zr abundance was derived from neutral lines whereas the Nd abundance came from ionized lines, and the Zr/Nd abundance ratio might be affected by gravity. This is not likely, however, as the Ba and CH stars with similar Zr/Nd ratios are much hotter, and this high ratio of heavier to lighter heavy elements is also found for other species in the Galactic stars.

The observed low (relative to predictions from exponential distributions of exposures) Zr/Nd ratio in the *s*-processed material of the AGB stars does help to account for the apparent excess of Nd (and other heavy elements) relative to Zr (and other lighter heavy elements) in the field stars; the AGB S stars are likely to be major donors of heavy elements to the SMC's interstellar medium. It may be that the anomalous ratio of the lighter heavy to the heavier heavy elements in the SMC owes its origin not to donation of *r*-process elements from supernovae but to the unusual (nonsolar) compositions of the AGB stars.

5.2.2. Rb *Abundance*

The Rb abundance through the branch at ^{85}Kr in the *s*-process path is a monitor of the neutron density at which the *s*-process operates in the He-shell (Tomkin & Lambert 1983). Models of intermediate-mass AGB stars predict the neutron density to increase with increasing core mass. At high core mass, $M_c \gtrsim 1.1\ M_\odot$, ^{85}Kr is expected to capture a neutron rather than decay and the Rb abundance (relative to Zr, for example) is predicted to be an order of magnitude more abundant than at the lower neutron densities achieved at lower core masses (see Beer & Macklin 1989). This link between Rb and core mass (and, hence, the total mass) lead us to extract the Rb abundance from the 7800 Å resonance line. Our attempt was frustrated and diverted by the weakness of the 7800 Å line and the remarkably low abundance of Rb in the supergiant N371:C12.

Comparison of observed and synthetic spectra of N371:C12 suggest [Rb/Fe] ≈ -1.3 and, as discussed in § 4.5, this abundance might be more properly considered as an upper limit because the Rb I line is not an obvious depression below the general level of the TiO absorption lines. This is a remarkable underabundance of Rb because [Zr/Fe] ≈ -0.2 for the same star. However, we note that the Zr/Nd ratio in the S-stars is well below that which characterizes the solar system ratio (§ 5.2.1). Also, studies of the field stars in the SMC by RB, SSF, and LL find nonsolar ratios of the heavy-to-light neutron-capture species. The underlying heavy-element abundance pattern in the SMC needs to be examined before we can interpret our Rb abundance.

RB, SSF, and LL provide abundances for the light *s*-process elements Y and Zr, the heavy *s*-process elements Ba, La, and Ce, Nd, representing a mixture of *r*- and *s*-process contributions, and three primarily *r*-process heavy elements Sm, Eu, and Gd. In Table 7 we present straight averages of RB, SSF, and LL for the heavy elements abundances in the SMC field. We present the abundances in both spectroscopic bracket notation, relative to the solar photospheric values (Anders & Grevesse 1989), and on the usual scale of log ϵ(H) = 12.0; also listed are the breakdown of these elements into *r*- and *s*-process contributions, as derived from solar-system abundances (Käppeler, Beer, & Wisshak 1989). In Figure 8 we plot the field SMC abundances versus the fraction of *r*-process contribution. Although the uncertainties are large, there are two interesting points to this figure: (1) the "*r*-process" species ($f_{r\text{-process}} > 0.5$) are overabundant relative to the "*s*-process" species ($f_{r\text{-process}} < 0.5$), and (2) the heavy *s*-process elements (Ce, Ba, and La) are overabundant relative to the light *s*-process elements (Y and Zr). The overabundance of the *r*-process species was discussed by Russell & Dopita (1992) and suggests that the relative contribution of *r*-process is larger in the SMC than in the solar

TABLE 7

AVERAGE HEAVY-ELEMENT ABUNDANCES IN THE SMC FIELD AND THEIR *r*- AND *s*-PROCESS FRACTIONS[a]

ELEMENT	[*X*/Fe][b]	log ϵ_{SMC}[b]	SOLAR SYSTEM FRACTIONS (*s*)	(*r*)
Y	-0.52 ± 0.15	1.72	0.68	0.32
Zr	-0.57 ± 0.14	2.03	0.77	0.23
Ba	-0.39 ± 0.53	1.74	0.79	0.21
La	-0.35 ± 0.25	0.87	0.72	0.28
Ce	-0.31 ± 0.22	1.24	0.89	0.11
Nd	-0.12 ± 0.20	1.38	0.42	0.58
Sm	$+0.05$	1.05	0.28	0.72
Eu	$+0.15$	0.66	0.03	0.97
Gd	-0.28	0.84	0.17	0.83

[a] As in the solar system, Käppeler, Beer, & Wisshak 1989.

[b] Straight averages of abundances from Luck & Lambert 1992, Russell & Bessell 1989, and Spite, Spite, & François 1989 relative to solar photospheric values (Anders & Grevesse 1989) and on the logarithmic scale where log ϵ(H) = 12.0.

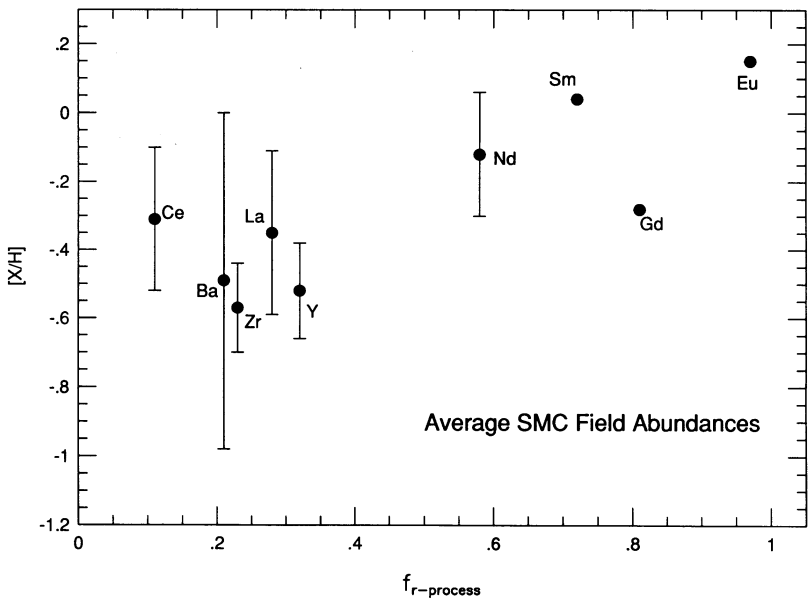

FIG. 8.—Heavy-element abundances in the field SMC stars versus the *r*-process contribution fraction (as in solar system, Käppeler, Beer, & Wisshak 1989). The abundances are straight averages from Luck & Lambert (1992), Russell & Bessell (1989), and Spite, Spite, & François (1989) relative to solar photospheric values. Note the apparent overabundance of "*r*-process only" elements.

neighborhood. The overabundance of Ce, Ba, and La relative to Y and Zr (relative to solar) is most easily explained by the *s*-process abundance distribution in the SMC being characterized by a larger neutron exposure than that which describes the solar *s*-process distribution of the main component ($\tau_0 = 0.30$ mb^{-1}). Note that a high neutron exposure will also increase the *s*-process contribution of elements such as Sm, Eu, and Gd.

With the possibility that the SMC exhibits heavy-elements abundances that may differ in both the neutron exposure and relative *s*- and *r*-process contributions, as well as the fact that our data are limited, we adopt the simplest approach to interpreting our abundances. We have already discussed the low Zr/Nd ratios in the luminous S-stars and suggested that the *s*-process in these stars is probably characterized by a large (extreme) exposure (and a low neutron density). The data from the field of the SMC also point to a larger *s*-process neutron exposure for the SMC in general. Using Malaney (1987b) extreme single-exposure model ($\tau = 1.3$ mb^{-1}), we compare in Figure 9 these predictions to the average Rb, Zr, and Nd *s*-process abundances of the S-stars: we have computed relative log $\epsilon(s)$ with equation (1) using N371:C12 as a standard. The agreement is very good; if our (uncertain) Rb abundances are adopted, the low Rb/Zr ratio requires a large neutron exposure at low neutron densities ($n_n \lesssim 10^8$ cm^{-3}). We can now see if this extreme neutron exposure can give a plausible fit to the underlying *s*-process abundances in N371:C12; such a comparison is fraught with the uncertainty of the relative *s*- and *r*-process contributions in the SMC. We show in the bottom panel of Figure 9 a comparison of log $\epsilon(s)$ in N371:C12 with the predictions of the $\tau = 1.3$ mb^{-1} model, assuming a solar mixture of *s*- and *r*-process. The comparison between model and observation is tolerable, especially when all the uncertainties are considered. Perhaps the best comparison is the Rb/Nd ratio, as both these elements contain similar *r*-process fractions (0.59 for Rb and 0.58 for Nd, in the solar system). The $\tau = 1.3$ mb^{-1} model predicts Rb/Nd = 0.32 while we derive Rb/Nd ≈ 0.5 for N371:C12. We note that, in order to get a more "reasonable" exposure, we could, within the error bars, increase the Rb/Zr ratio in the *s*-processed material of the S-stars. To do that, we could (1) increase the Rb/Fe ratio; this would diminish the *r*-process contribution for Rb (as seen in N371:C12), and conflicts with the idea of a larger contribution of the *r*-process in the SMC and (2) decrease the Zr/Fe ratio; the Zr/Nd ratio further decreases, which calls for a higher exposure.

Solar metallicity Galactic S-stars show a solar-system distribution of *s*-process elements (Smith & Lambert 1990b). However, we note that the Galactic S-star HD 35155 shows a similar abundance pattern to the SMC AGB stars. In Figure 10, we show again log $\epsilon(s)$ for the SMC AGB stars (top panel) with a $\tau = 1.3$ mb^{-1} model and the same quantities for HD 35155 (bottom panel), with the abundances taken from Smith & Lambert (1990b) and Lambert & Smith (1993). The *s*-process abundance ratios in HD 35155 are, within the uncertainties, the same as those in the SMC AGB stars. HD 35155 and the SMC stars also have the same metallicity ([Fe/H] ≈ -0.5). This demonstrates that the *s*-process operating in the SMC ABG stars is not peculiar to the SMC itself, but is more probably merely a function of the overall metallicity. It should be mentioned that HD 35155 is a binary star with a white dwarf companion and its large *s*-process overabundances are the result of mass transfer when the white dwarf was a TP-AGB star (Smith & Lambert 1988, 1990b; Brown et al. 1990). This does not influence the above comparison. The current abundance pattern on HD 35155 reflects the abundances in the former AGB star in the system.

5.3. *Envelope Burning*

As discussed in § 1, two observable signatures of envelope burning are a low $^{12}C/^{13}C$ ratio from H-burning by the CN-cycle and a ^{7}Li enrichment from consumption of ^{3}He by the ^{7}Be-transport mechanism. In this section, we relate our observations of $^{12}C/^{13}C$, [C/H] and the Li abundances to predictions for envelope burning.

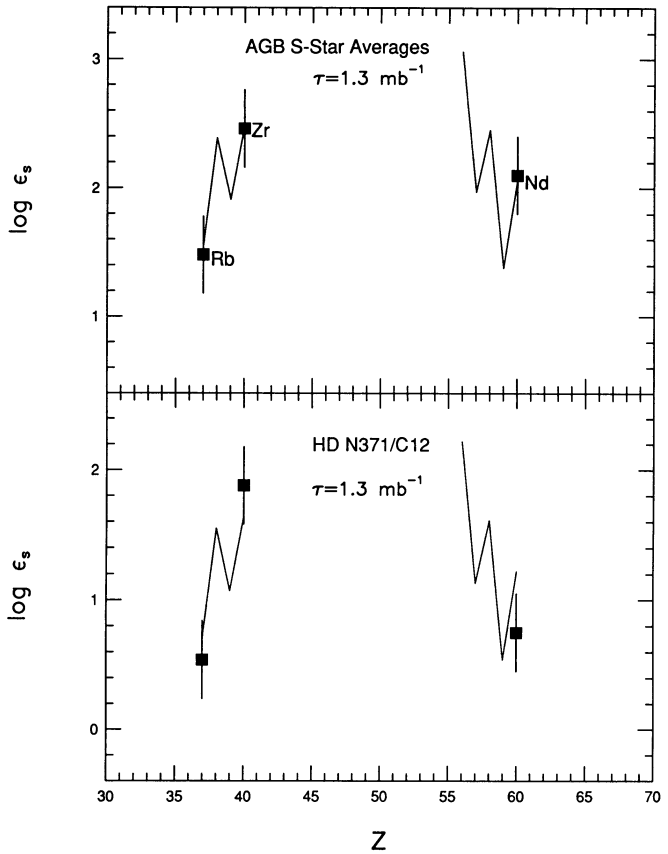

FIG. 9

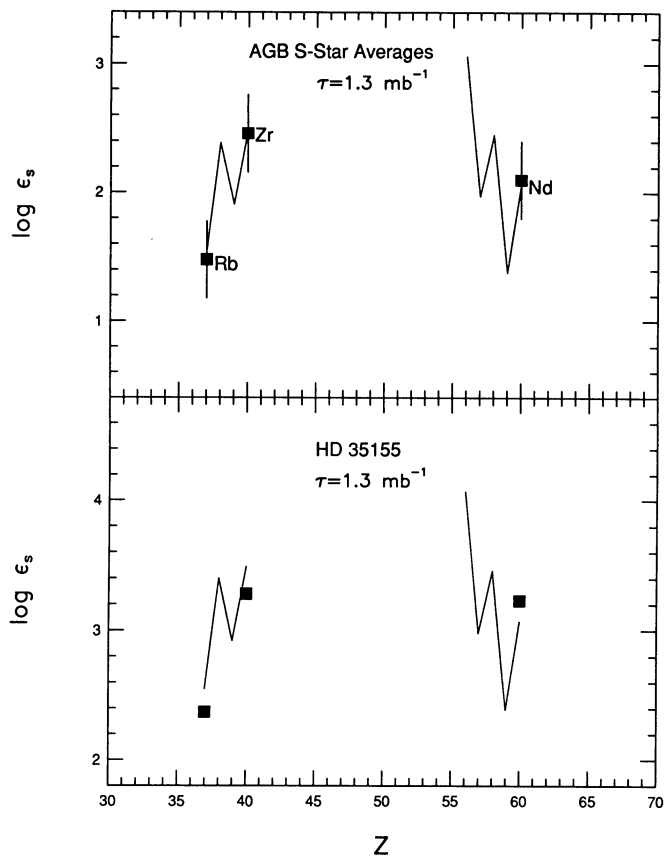

FIG. 10

FIG. 9.—Observed Rb, Zr, and Nd abundances and *s*-process single-exposure model predictions with $\tau = 1.3$ mb^{-1} (Malaney 1987b). *Upper panel*: in the *s*-processed material in the luminous S-stars. Lower panel: in the reference supergiant N371:C12, after subtraction of an assumed solar *r*-process fraction. Error bars reflect a ± 0.5 dex uncertainty in the abundances (abundance scale arbitrary).

FIG. 10.—Observed Rb, Zr, and Nd abundances and *s*-process single-exposure model predictions with $\tau = 1.3$ mb^{-1} (Malaney 1987b). *Upper panel*: in the *s*-processed material in the luminous S-stars. *Lower panel*: in the Galactic S-star HD 35155. For clarity, error bars are omitted for HD 35155, Although expected conservative uncertainties would be ± 0.3 dex (abundance scale arbitrary).

The primary evidence for H-burning is the low $^{12}C/^{13}C$ ratio found in all four examined S stars ($^{12}C/^{13}C \approx 7 \pm 3$) but a higher ratio ($^{12}C/^{13}C \approx 25$) in the supergiant. The latter is consistent with predictions for a cool supergiant following its first dredge-up. The initial $^{12}C/^{13}C$ ratio of the stars is not known but $^{12}C/^{13}C \approx 80$ is a fair guess and consistent with $^{12}C/^{13}C \approx 25$ in a supergiant after the first dredge-up. The much lower ratios of the S stars indicate severe contamination of their atmospheres with H-burning products. Until the $^{12}C/^{13}C$ ratios of less luminous AGB stars are measured, it can only be surmised that the low $^{12}C/^{13}C$ ratios of the S stars are due to envelope burning and not to an earlier phase of stellar evolution.

Interpretation of the carbon abundances is compromised somewhat by the uncertainty over the initial abundance for these stars. Russell & Dopita (1992) give [C/H] = −0.60 for F-type supergiants in the SMC. Pagel (1993) in a review of stellar and interstellar (H II regions) abundances notes that [C/H] ≈ −0.6 is provided by F- and K-supergiants as well as B stars but, as earlier noted by Russell & Bessell (1989), the H II regions give a lower abundance of [C/H] ≈ −1.2. If the stellar abundance of [C/H] = −0.6 is adopted, the C abundance of the supergiant N371:C12, [C/H] = −1.1, is approximately consistent with the prediction for a star after the first dredge-up.

The S stars are at luminosities at which carbon stars are expected in the absence of envelope burning. We suppose that envelope burning has converted C to N and reduced the C/O ratio to just below unity. Since the O abundance of the SMC is [O/H] ≈ −0.7 (Russell & Dopita 1992), and the O abundance is not expected to be reduced in these evolved stars, a ratio C/O ≈ 0.9 implies [C/H] ≈ −0.5. Our estimated [C/H] for HV 11223 is approximately consistent with this estimate. The three other estimates, especially [C/H] = −1.8 for HV 12179, cannot be reconciled with our assumption that the initial O abundance is approximately preserved in AGB stars and the general assertion that C/O is just less than unity for S stars. Inspection of our spectra at 6930 Å show no evidence of the ZrO γ(1–0) absorption band in any of the stars. The strong TiO bands and the weak (or absent) ZrO band are consistent with the inferred Zr/Ti ratio from our abundance analysis and the low C/O ratio. Brett (1991) also found C/O ratios significantly lower than 1 in his low-resolution study of luminous AGB stars in the SMC.

Production of Li in AGB stars is ascribed to the ^{7}Be-transport mechanism (Cameron & Fowler 1971) in which ^{3}He is converted to ^{7}Li via the reaction chain ^{3}He(^{4}He, γ)^{7}Be(e, ν)^{7}Li. Lithium production by envelope burning was first demonstrated in some detail by SDU. Recently, Sackmann & Boothroyd (1992) predicted ^{7}Li synthesis from envelope burning in a "fully self-consistent"

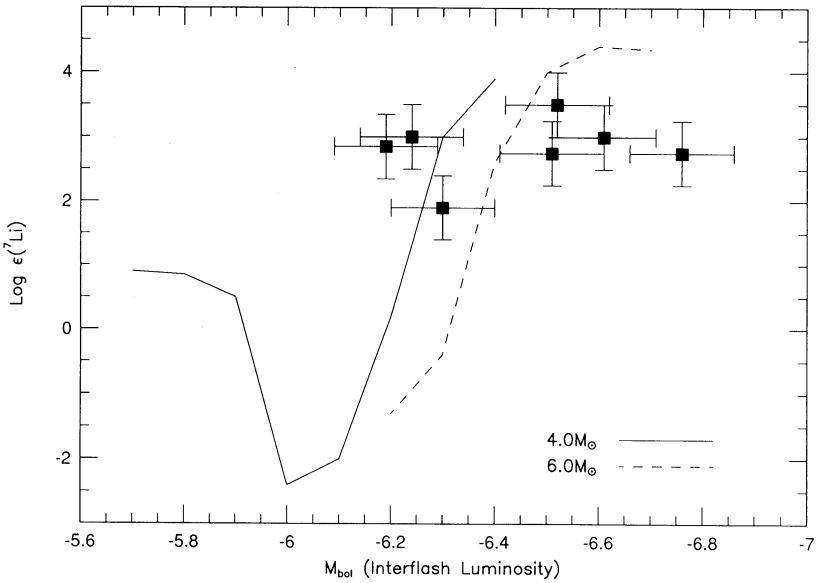

FIG. 11.—Li abundance vs. M_{bol} compared to the models of Sackmann & Boothroyd (1992). The observed abundances are straight averages of our determinations for the 6707 Å and the 8126 Å lines, and the error bars are estimated uncertainties of ± 0.5 dex in log ϵ(Li) and ± 0.1 in M_{bol}.

evolutionary sequence of luminous AGB stars of 3–7 $M_\odot$ and of two initial metallicities ($Z = 0.02$ and 0.001) spanning the SMC metallicity $Z = 0.005$. The supply of ^{3}He in the convective envelope was manufactured in the main-sequence stars which generate a ^{3}He-rich zone outside the layers in which H-burning generates the stellar luminosity. In the model sequences considered by Sackmann & Boothroyd, the synthesis of ^{3}He was followed in detail as the sequences were begun with stars on the Hayashi track prior to the main sequence.

Sackmann & Boothroyd's sequences of AGB stars predict that Li-rich AGB stars will have a mass range of 5 to 7 $M_\odot$ for $Z = 0.02$ and 4 to 7 $M_\odot$ for $Z = 0.001$ with peak Li abundance of log ϵ(Li) ≈ 4.5 attained at luminosity $M_{bol} \approx -6.2$ to -6.8. A comparison of these predictions and the observed properties of the SMC Li-rich stars (Fig. 11) shows at once, as Sackmann & Boothroyd (1992) noted, that the observed and predicted luminosities of the Li-rich stars are in excellent agreement.

The agreement is less satisfactory for the Li abundances. Sackmann & Boothroyd predict log ϵ(Li) ≈ 4 to 4.5 for the maximum abundance but our inferred abundances are log ϵ(Li) ≈ 3 for six of the seven stars. The lower abundance for HV 11366 is consistent with the predictions because some stars at a given luminosity have yet to achieve the maximum Li abundance, and others may have begun to show a declining Li abundance as ^{3}He has been exhausted. We do not think our sample is at all atypical of the Li-rich stars in the SMC. Our low-resolution survey (Smith et al. 1993) does not suggest that there are many stars with log ϵ(Li) ≈ 4–4.5 rather than the present sample's log ϵ(Li) ≈ 3. On the other hand, Sackmann & Boothroyd note that published Li abundances for Galactic Li-rich N and S stars span and exceed the predicted range of Li abundances.

Several reasons might be advanced for supposing that the predicted abundances could be reduced. Sackmann & Boothroyd suggest (see also SDU) that a lower temperature at the base of the convective envelope will result in a reduced Li abundance. The necessary lower temperature might be achieved with more accurate opacities. If this adjustment were metallicity dependent, the difference between the maximum Li abundances [log ϵ(Li) ≈ 3.0] of the SMC Li-rich and Galactic [log ϵ(Li) ≈ 4–5.5] Li-rich stars might be explained. It seems, however, that the inclusion of better (higher) opacities in the stellar envelope will increase the temperature of the base of the convective envelope (Sackmann & Boothroyd 1991). Alternatively, the efficiency of the ^{7}Be-transport mechanism may have been overestimated by Sackmann & Boothroyd, i.e., convection may transport the ^{7}Be less rapidly away from the base of the convective envelope. Also, the Li abundance is related to the initial ^{3}He abundance. Some Galactic 4–7 $M_\odot$ supergiants have a ^{12}C/^{13}C ratio much less than that predicted by the first dredge-up. Since production of ^{13}C may result in destruction of the ^{3}He reservoir, it is possible that Li-rich AGB stars will have a smaller Li abundance as a result of the lower ^{3}He abundance. We note that Brown et al. (1993) have also calculated hot bottom burning envelope models. In Figure 12 we compare our Li abundances with some of the model predictions of Brown et al. (1993). The agreement is better than with the Sackmann & Boothroyd (1992) predictions. The differences between the two sets of predictions can be attributed to the use of different opacities, of different convection formalisms, and to the construction of self-consistent stellar models by Sackmann & Boothroyd whereas Brown et al. only calculated envelope models.

How efficient a source of Li luminous AGB stars are for the interstellar medium may be estimated using Clayton's (1984) analytical galactic chemical evolution model. Clayton's model assumes that the star formation is linearly proportional to the mass of gas. If the infall of gas is neglected (" closed box " approximation), the Li abundance of the ISM saturates at

$$\epsilon(\mathrm{Li})_{max} = \epsilon(\mathrm{Li})_{AGB} \frac{R(m_{low}, m_{up})}{R(m_l, \infty)}, \quad (2)$$

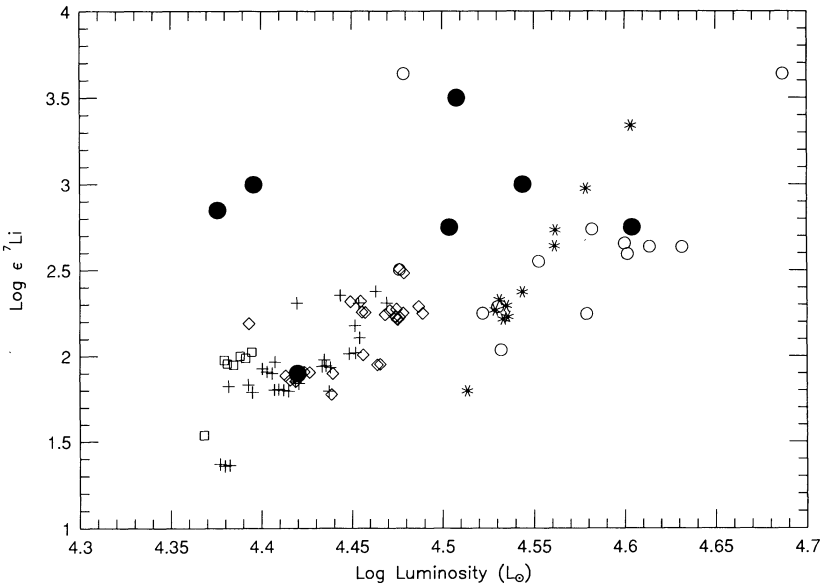

FIG. 12.—Li abundance vs. M_{bol} compared to models from Brown et al. (1993). The models have a solar composition. A decreased metallicity will shift the points to lower luminosities, and the agreement between models and observations will improve. *Filled circles*: observations. *Open squares*: models with 4.5 $M_\odot$; *crosses*: 5.0 $M_\odot$; *diamonds*: 5.25 $M_\odot$; *stars*: 6.0 $M_\odot$; *open circles*: 6.5 $M_\odot$.

where only AGB stars of mass $m_{low} \leq M \leq m_{up}$ return Li to the ISM, and $R(m_a, m_b) = \int_{m_a}^{m_b} (m - w_m)\phi(m)d(m)$ is the mass of ejecta returned to the ISM by stars in the range $m_a \leq M \leq m_b$, with a core mass w_m; m_l is the present turn-off mass. Taking $m_{low} = 4\ M_\odot$ and $m_{up} = 7\ M_\odot$, $m_l = 1\ M_\odot$, and $w_m = 0.7\ M_\odot$ for stars of mass $M \leq 7\ M_\odot$ and $w_m = 1.4\ M_\odot$ for stars of mass $M > 7\ M_\odot$, we find $R(4, 7)/R(1, \infty) \approx 0.2$, using Tinsley's (1980) IMF. With our log $\epsilon(\mathrm{Li})_{AGB} \approx 3.0$, the ISM (and hence young stars) Li abundance should be log $\epsilon(\mathrm{Li})_{ISM} \approx 2.3$. On the other hand, if we demand log $\epsilon(\mathrm{Li})_{ISM} \approx 3.3$, log $\epsilon(\mathrm{Li})_{AGB} \approx 4.0$ is required, if stars of 4 $M_\odot < M < 7\ M_\odot$ are the dominant Li source in the SMC. If m_{low} is reduced to 1 $M_\odot$ and $\epsilon(\mathrm{Li})_{AGB}$ is assumed to be independent of stellar mass, log $\epsilon(\mathrm{Li})_{ISM} \approx 2.85$ is expected for log $\epsilon(\mathrm{Li})_{AGB} \approx 3.0$. Of course, current models of envelope burning stars predict that Li synthesis is confined to stars with $M \gtrsim 4\ M_\odot$. The Li abundance of the SMC's ISM is unknown. For the Galaxy, log ϵ(Li) is 3.0–3.3 which, in the context of Clayton's model, may be achieved only if either $\epsilon(\mathrm{Li})_{AGB}$ is substantially higher than our measurements of Li in SMC's AGB stars or the major supplier of Li is not AGB stars but, for example, Type II supernovae (see Woosley et al. 1990 on the ν-process).

6. CONCLUSIONS

This analysis has examined the detailed derivation of key elemental abundances in a sample of luminous SMC S-stars, with relatively strong Li I lines, and compared these abundances to an SMC M-supergiant in a different evolutionary phase (hydrostatic core burning). The operation of the *s*-process and third dredge-up is shown clearly in a comparison of the Zr and Nd abundances in the S stars with those in the supergiant. The *s*-process ratio of Zr/Nd in the SMC S-stars is quite low when compared to solar system material and suggests a large neutron exposure in these stars. When taken with the rather low Rb abundances in these stars, the best fit to the Rb, Zr, and Nd *s*-process abundances requires both a large neutron exposure ($\tau \approx 1.3$ mb^{-1}) and a low neutron density ($N_n = 10^8$ cm^{-3}). These results are not peculiar to the SMC, however, as Galactic S, Ba, and CH stars at the SMC's metallicity ([Fe/H] ≈ -0.5) exhibit similar *s*-process abundance ratios. This decrease of the lighter *s*-process elements, such as Rb or Zr, relative to the heavier nuclei, such as Nd, with decreasing [Fe/H] is in qualitative agreement with the expected behavior of the ^{13}C(α, n)^{16}O neutron source as discussed by Clayton (1988). These S stars represent almost the limit of AGB luminosities ($M_{bol} \gtrsim -7.1$) and would indicate stars with large core masses (We recall, however, that the masses of the SMC AGB stars are ill determined). If ^{22}Ne(α, n)^{25}Mg does not operate in these stars, there may not be many AGB candidates left for the ^{22}Ne source.

We note that in Galactic disk F dwarfs, the Zr/Nd ratio is constant down to at least [Fe/H] $= -0.7$ (Edvardsson et al. 1993). This difference between evolved and unevolved low-metallicity stars might be due to a larger contribution of the weak *s*-process at low metallicity (which would bring the Zr abundance up), or to an *r*-process contribution with different abundance ratios than in the solar system material, or to the fact that AGB stars with [Fe/H] ≈ -0.5 do not dominate in the heavy-element contribution to the unevolved stars at the same metallicity. We may also speculate that the Galactic Ba, CH, and extrinsic S stars heavy element abundances, from which we derive the Galactic Zr/Nd ratio at [Fe/H] less than solar, are a distorted version of an AGB abundance pattern (the result of gas-dust separation in the accretion process?).

Li is found in the seven AGB stars to exist at typical abundances of log ϵ(Li) ≈ 3.0 (Li/H $\approx 10^{-9}$): this is much larger than expected from standard AGB evolution (where Li has been destroyed and/or diluted due to convection) and betrays the presence of envelope burning. The low ^{12}C abundances ([^{12}C/H] ≈ -1.0) and ^{12}C/^{13}C ratios (^{12}C/^{13}C $\approx$ 5–9) also agree with what is expected

from envelope burning. These results are in rough agreement with the models of Sackmann & Boothroyd (1992) and Brown et al. (1993), although there is still uncertainty in both the model predictions and the derived Li abundances.

We thank G. Bazan for useful discussions and for providing results prior to publication. This work is supported in part by the NSF (AST 91-15090) and the Robert A. Welch Foundation of Houston, Texas.

REFERENCES

Anders, E., & Grevesse, N. 1989, Geochim. Acta, 53, 197
Bazan, G., & Lattanzio, J. 1992, in Nuclei in the Cosmos, ed. F. Käppeler & K. Wisshak (Bristol: Inst. of Physics), 521
Beer, H., & Macklin, R. L. 1989, ApJ, 339, 962
Blanco, V. M., McCarthy, M. F., & Blanco, B. M. 1980, ApJ, 242, 938
Blöcker, T., & Schönberner, D. 1991, A&A, 244, L43
Boothroyd, A. I., & Sackmann, I.-J. 1992, ApJ, 393, L21
Brown, J. A., Smith, V. V., Lambert, D. L., Dutchover, E., Jr., Hinkle, K. H., & Johnson, H. R. 1990, AJ, 99, 1930
Brown, L. E., Bazan, G., Clayton, D. D., & Truran, J. W. 1993, in preparation
Brett, J. M. 1991, MNRAS, 249, 538
Busso, M., Picchio, G., Gallino, R., & Chieffi, A. 1988, ApJ, 326, 196
Cameron, A. G. W., & Fowler, W. A. 1971, ApJ, 164, 111
Chackerian, C., Jr., & Tipping, R. H. 1983, J. Molec. Spectrosc., 99, 431
Clayton, D. D. 1984, ApJ, 285, 411
———. 1988, MNRAS, 234, 1
Dale, R. M., Herman, M., Johns, J. W. C., McKellar, A. R. W., Nagler, S., & Strathy, I. K. M. 1979, Canadian J. Phys., 57, 677
Davis, S. P., & Phillips, J. G. 1963, The Red System of the CN Molecule (Berkeley: Univ. of Calif. Press)
Doverstål, M., & Weijnitz, P. 1992, Molec. Phys., 75, 1375
Edvardsson, B., Andersen, J., Gustafsson, B., Lambert, D. L., Nissen, P. E., & Tomkin, J. 1993, A&A, 275, 101
Fuhr, J. R., Martin, G. A., & Wiese, W. L. 1988, J. Phys. Chem. Ref. Data, 17, Suppl. 4
Gratton, R. G., & Sneden, C. 1987, A&A, 178, 179
Gustafsson, B., Bell, R. A., Eriksson, K., & Nordlund, Å. 1975, A&A, 42, 407
Holweger, H., Heise, C., & Kock, M. 1990, A&A, 232, 510
Holweger, H., & Müller, E. A. 1974, Sol. Phys., 39, 19
Hughes, S. M. G. 1989, AJ, 97, 1634
Iben, I., Jr., 1973, ApJ, 185, 209
———. 1975, ApJ, 196, 525
———. 1981, ApJ, 243, 987
Iben, I., Jr., & Renzini, A. 1983, ARA&A, 21, 271
Jøgensen, U. G. 1992, Rev. Mexicana Astron. Af., 23, 195
Jørgensen, U. G., & Larsson, M. 1990, A&A, 238, 424
Käppeler, F., Beer, H., & Wisshak, K. 1989, Rep. Progr. Phys., 52, 945
Kovacz, V. 1985, A&A, 150, 232
Kurucz, R. L. 1989, private communication
Kurucz, R. L., Furenlid, I., Brault, J., & Testerman, L. 1984, Solar Flux Atlas from 296 to 1300 nm (Cambridge: Harvard Univ. Press)
Kurucz, R. L., & Peytreman, E. 1975, SAO Spec. Rep., No. 362
Lambert, D. L., Brown, J. F., Hinkle, K. H., & Johnson, H. R. 1984, ApJ, 284, 223
Lindgren, B. 1991, private communication
Lambert, D. L., & Smith, V. V. 1993, in preparation
Luck, R. E., & Bond, H. E. 1991, ApJS, 77, 515
Luck, R E., & Lambert, D. L. 1982, ApJ, 256, 189
———. 1992, ApJS, 79, 303 (LL)
Malaney, R. A. 1987a, Ap&SS, 137, 251
———. 1987b, ApJ, 321, 832
Pagel, B. E. J. 1993, in New Aspects of Magellanic Cloud Research, ed. B. Baschek, G. Klare, & J. Lequex (Berlin: Springer), 330
Phillips, J. G. 1988, private communication
Plez, B. 1990, Mem. Soc. Astron. Ital., 61, 765
Plez, B., Brett, J. M., & Nordlund, Å. 1992, A&A, 256, 551
Rebeirot, E., Azzopardi, M., & Westerlund, B. E. 1993, A&AS, 97, 603
Renzini, A., & Voli, M. 1981, A&A, 94, 175
Ridgway, S. T., Joyce, R. R., White, N. M., & Wing, R. F. 1980, ApJ, 235, 126
Russell, S. C. 1993, in The Feedback of Chemical Evolution on the Stellar Content of Galaxies, ed. D. Alloin, & G. Stasinska (Obs. de Paris), in press
Sackmann, I.-J., & Boothroyd, A. I. 1991, ApJ, 366, 529
———. 1992, ApJ, 392, L71
Sackmann, I.-J., Smith, R. L., & Despain, K. H. 1974, ApJ, 187, 126
Sanders, R. H. 1967, ApJ, 150, 971
Scalo, J. M., Despain, K. H., & Ulrich, R. K. 1975, ApJ, 196, 805 (SDU)
Scalo, J. M., & Ulrich, R. K. 1973, ApJ, 183, 151
Scholz, M. 1992, A&A, 253, 203
Schwarzschild, M., & Härm, R. 1967, ApJ, 150, 961
Smith, V. V. 1984, A&A, 132, 326
———. 1993, in Nuclei in the Cosmos, ed. F. Käppeler & K. Wisshak (Bristol: Inst. of Physics), 17
Smith, V. V., & Lambert, 1985, ApJ, 294, 326
———. 1986, ApJ, 311, 843
———. 1988, ApJ, 333, 219
———. 1989, ApJ, 345, L75
———. 1990a, ApJ, 361, L69
———. 1990b, ApJS, 72, 387
Smith, V. V., Lubowich, D., Plez, B., & Lambert, D. L. 1993, in preparation
Smith, V. V., & Suntzeff, N. B. 1987, AJ, 93, 359
Sneden, C. 1973, Ph.D. thesis, Univ. of Texas at Austin
Spite, F., & Spite, M. 1991, in The Magellanic Clouds, ed. R. Haynes & D. Milne (Dordrecht: Kluwer), 243
Spite, F., Spite, M., & François, P. 1989, A&A, 210, 25 (SSF)
Sweigart, A. V. 1974, ApJ, 189, 289
Thévenin, F., Jasniewicz, G. 1992, A&A, 266, 85
Tinsley, B. A. 1980, Fund. Cosmic. Phys., 5, 287
Tomkin, J., & Lambert, D. L. 1983, ApJ, 273, 722
———. 1986, ApJ, 311, 819
Truran; J. W., & Iben, I., Jr. 1977, ApJ, 216, 797
Ulrich, R. K. 1973, in Explosive Nucleosynthesis, ed. D. N. Schramm & D. W. Arnett (Austin: Univ. of Texas Press), 139
Uus, U. 1973, Soviet Astron., 17, 196
Vanture, A. D. 1992, AJ, 104, 1997
Westerlund, B., Olander, N., Richer, H. B., & Crabtree, D. R. 1978, A&AS, 31, 61
Wood, P. R. 1990, From Miras to Planetary Nebulae, ed. M. O. Mennessier & A. Omont (Gif-sur-Yvette: Editions Frontières), 67
Wood, P. R., Bessell, M. S., & Fox, M. W. 1983, ApJ, 272, 99 (WBF)
Wood, P. R., Moore, G. K. G., & Hughes, S. M. G. 1991, in The Magellanic Clouds, ed. R. Haynes & D. Milne (Dordrecht: Kluwer), 259
Woosley, S. E., Hartmann, D. H., Hoffman, R. D., & Haxton, W. C. 1990, ApJ, 356, 272